Ca^{2+}-Mediated Thermal Sensing in Plants

by

Yan Xue

Department of Biology
Duke University

Date:_____
Approved:

_____
Zhenming Pei, Supervisor

_____
Philip Benfey

_____
Xinnian Dong

_____
Jorg Grandl

_____
Vikas Bhandawat

Dissertation submitted in partial fulfillment of the requirements for the degree of Doctor of Philosophy in the Department of Biology in the Graduate School of Duke University

2017

ABSTRACT

Ca^{2+}-Mediated Thermal Sensing in Plants

by

Yan Xue

Department of Biology
Duke University

Date:_____

Approved:

_____
Zhenming Pei, Supervisor

_____
Philip Benfey

_____
Xinnian Dong

_____
Jorg Grandl

_____
Vikas Bhandawat

An abstract of a dissertation submitted in partial fulfillment of the requirements for the degree of Doctor of Philosophy in the Department of Biology in the Graduate School of Duke University

2017

Abstract

Temperature is an omnipresent environmental factor that shapes the growth, development and survival of plants. However, global warming has been an inevitable process and caused unusual temperature patterns across the world. As a consequence, forestry as well as agricultural plants are reportedly facing challenges from their environment. Several temperature responses in plant have been described, including short-term responses (such as acclimation) that increase tolerance towards sudden temperature stresses; as well as long-term responses (for example vernalization and flowering) that adjust growth and development to cope with seasonal temperature changes. However, the molecular mechanisms of how plants perceive temperature changes remain poorly understood. It has been observed for decades that one earliest response of plants towards low temperature is a transient increase of the cytosolic free Ca^{2+} concentration ($[Ca^{2+}]_i$). Considering the highly conserved role of $[Ca^{2+}]_i$ increases in mediating thermal perception in animals, it has been speculated that $[Ca^{2+}]_i$ increases may also play a role in thermal perception in plants. Nevertheless, despite intensive efforts, the molecular components responsible for cold-induced $[Ca^{2+}]_i$ increases remain elusive. In this study, we carried out Ca^{2+}-imaging-based forward genetic screen in *Arabidopsis thaliana*, isolated mutants defective in cold-induced $[Ca^{2+}]_i$ increases (*coca*) and identified corresponding genes responsible for the *coca* phenotype through physical mapping. One of the mutants, named

coca1, is highly specific to low temperature perception versus other stimuli, including osmotic, ionic and oxidative stimuli. *coca1* displays compromised cold-induced [Ca^{2+}] increases in both cotyledons and roots, as well as reduced growth fitness under ambient cool temperature. *COCA1* encodes the dynamin-related protein 1A (DRP1A) and is localized on the plasma membrane. Our pharmacological studies showed that DRP1A acts upstream of plasma membrane rigidification and may mediate temperature perception by modification of membrane curvature which in turn opens Ca^{2+} channels. Alternatively, DRP1A may regulate endocytosis and channel activity through endocytosis signaling. Identification of *coca1* as the first *Arabidopsis* mutant defective in cold-induced $[Ca^{2+}]_i$ increases and DRP1A as a key player in thermal perception will greatly extend our understanding of plant adaptation to temperature changes, open up new avenues for studying Ca^{2+} signaling towards other stimuli and provide potential molecular genetic targets for engineering cold-resistant crops.

Dedication

First of all, I would like to thank my supervisor Zhenming Pei. I would like to let you know that I am grateful for your trust and support throughout my whole Ph.D. study. It has been a long and tough journey with ups and downs. Thank you for being always patient and encouraging even during the difficult times when the project does not progress as expected. Through this the past over 7 years, I learnt a lot from you regarding sciences as well as beyond sciences, which I will benefit for sure for the rest of my life.

Then I would like to thank my labmate Fang Yuan. Thank you for your suggestions on the project, your friendship and your unconditional strong support. Your determination and fearlessness towards difficulties influenced and inspired me. I feel appreciated to be able to work with you and learn from your attitude.

I would also like to thank all my committee members, Dr. Xinnian Dong, Dr. Philip Benfey, Dr. Jorg Grandl and Dr. Vikas Bhandawat, as well as Dr. Pelin Volkan, who is not on my committee, but has been so supportive and encouraging. Thank you all for your critical suggestions on the project. Thank you for spending your time meeting and talking with me about my future career. I sincerely appreciate you all and your suggestions.

I would also like to express my gratitude to my friends, especially Qingyun Li, Liana Burghardt, Alejandro Pietrek, Xuan Huang, Feng Liu, Will Cook, Julia Shields, Benjamin Busch and Patrick Tang. I always feel it amazing that there are

so many people in the world, but for this or that reason, we get to know each other a little more than average so that we become friends. I appreciate every single moment I share with you. Durham feels home to me because of you.

Last but not least, I would like to thank my mom for loving me regardless of who and where I am. Thank you for always telling me I should go wherever I want and do whatever I like. I can be myself and not afraid of anything because I know you are home and I always have a home. You are my strongest support and my foundation of security where all the rest is built on. I owe you my whole life.

Table of Content

List of Tables

List of Figures

List of Abbreviations

COCA	Cold induced calcium increase
$[Ca^{2+}]_i$	Cytosolic free calcium concentration
PIF	PHYTOCHROME INTERACTING FACTOR
WT	Wild type
FLC	FLOWERING LOCUS C
FT	FLOWERING LOCUS T
SOC1	SUPPRESSOR OF OVEREXPRESSION OF CONSTANS 1
TAA	TRYPTOPHAN AMINOTRANSFERASE OF ARABIDOPSIS
SAURs	SMALL AUXIN UP RNAs
VRN	VERNALIZATION
VIN3	VERNALIZATION INSENSITIVE 3
COR	COLD RESPONSIVE GENES
LEA	LATE EMBRYOGENESIS ABUNDANT
CBF	C REPEAT BINDING FACTOR
ICE1	INDUCER OF CBF3 EXPRESSION 1
PRR	PSEUDORESPONSE REGULATOR
CCA1	CIRCADIAN CLOCK ASSOCIATED 1
LHY	LATE ELONGATED HYPOCOTYL
TOC	TIMING OF CAB1 EXPRESSION
GI	GIGANTEA
CK2	CASEIN KINASE 2
DMSO	Dimethyl sulfoxide
BA	Benzyl alcohol
EGTA	Ethylene glycol-bis(β-aminoethyl ether)-N,N,N',N'-tetraacetic acid
CNGC	Cyclic nucleotide gated calcium channel
EMS	Ethyl methanesulfonate
COCA	Cold induced $[Ca^{2+}]_i$ increases
FRET	Fluorescence resonant energy transfer

Chapter 1 Introduction

Temperature is one of the major environmental factors that shape the growth, development and survival of plants, including forestry and agricultural plants. However, global warming has been an inevitable process attributed to large scale of fossil fuel combustion. The observed and expected consequences of global warming include sea level rise as well as altered patterns of precipitation and temperature globally[1]. Plants, as sessile organisms, are more vulnerable to environmental changes. Studies show that up to half of European plant species would extinct or be threatened by 2080[2] due to global warming, with precipitation and temperature being the biggest impacts. Furthermore, according to the United Nation, global warming could lead to a loss of 2%, or 4.4 million metric tons of food annually, further exacerbating the worldwide food crisis. It is therefore important to understand how plants sense and respond to temperature changes.

1.1 Temperature mediated plant growth and development

Plants have colonized a wide range of environment throughout evolution. Species from polar and subpolar areas evolved specialized mechanisms to survive freezing temperatures. Species from tropical and subtropical areas are susceptible to cold[3,4] and those originated from temperate areas, including *Arabidopsis thaliana*, are able to sense a wide range of temperatures and develop a variety of physiological responses correspondingly. Among these responses, the best

understood include temperature mediated architectural growth, vernalization, cold acclimation and temperature entrained circadian clock.

1.1.1 Temperature mediated architectural changes

Temperature is known to mediate plant growth and development. Plants grown at warm temperature display characteristic morphological changes collectively called "thermomorphogenesis"[5]. Elongation of hypocotyl is one of the earliest thermomorphogenic responses[5]. It is believed to elevate the fragile meristem as well as photosynthetic cotyledons above the heated ground and facilitate cooling by providing better access to moving air[6]. In addition, petiole elongation occurs in both cotyledons and rosette leaves, along with an upward movement, called leaf hyponasty. Evidences show that plants displaying longer petioles and leaf hyponasty have higher transpiration rate and thus cooler leave[7]. Because these phenotypes largely mimic shade grown plants where PHYTOCHROME INTERACTING FACTORs (PIFs) play a critical role, the involvement of PIFs in plant thermomorphogenesis was investigated.

Studies on *pif4* mutant show that PIF4 is required for thermomorphogenesis[8,9]. Mutant *pif4* grown at 27°C phenocopies wild type (WT) plants grown at 22°C, including shorter hypocotyl and petiole length, as well as the absence of leaf hyponasty. Further studies show that PIF4 mediated thermomorphogenesis is at least partly achieved through activation of auxin biosynthesis. PIF4 binds to the promoters of auxin biosynthesis genes

TRYPTOPHAN AMINOTRANSFERASE OF ARABIDOPSIS (TAA) and *CYP79B2* in a temperature dependent manner and thereby activate auxin biosynthesis at high temperature[8]. In line with this observation, warmth induction of auxin responsive genes including *SMALL AUXIN UP RNAs* (*SAURs*) is abolished in *pif4* mutant. In addition, PIF4 itself is stabilized at warm temperature, because of the inactivation of its negative regulator PhyB[10]. Interaction with PhyB targets PIF4 for ubiquitination and subsequently proteasome mediated degradation. Therefore, warmth inactivation of PhyB results in increased amount of PIF4, which further intensify the auxin biosynthesis.

1.2.2 Vernalization

Vernalization is a process during which plants acquire competence of flowering after a prolonged exposure to cold[11]. Vernalization prevents the exposure of reproductive organs to freezing temperatures in winter and ensures that flowering occurs under favorable conditions in spring[12].

It is known that vernalization is achieved through epigenetic modification and subsequently silencing of *FLOWERING LOCUS C* (*FLC*) expression[13]. FLC represses the expression of *FLOWERING LOCUS T* (*FT)* and *SUPPRESSOR OF OVEREXPRESSION OF CONSTANS 1* (*SOC1*), which function as flowering integrators that coordinate the expression of floral meristem identity genes. Therefore, vernalization is a de-repressing process that removes the inhibition of floral transition.

To understand the molecular mechanism of vernalization induced epigenetic modification, forward genetic screen of mutants insensitive to vernalization was carried out, leading to the identification of components including VERNALIZATION 2 (VRN2), VRN5 and VERNALIZATION INSENSITIVE 3 (VIN3)[12,14-16]. It is now known that VRN2 is constitutively present on *FLC* chromatin. Cold triggers the binding of VIN3 to the first intron of *FLC*, which in turn recruits VRN5. When plants are returned to warm temperatures, indicating a favorable condition in spring for flowering, VRN5 binding will spread throughout *FLC* chromatin, leading to the silencing of *FLC*. As a result of FLC silencing, floral integrators *FT* and *SOC1* are de-repressed, leading to the transition of meristem into flowering tissues.

1.1.3 cold acclimation

One of the best studied temperature responses is cold acclimation, a process during which plants acquire resistance towards freezing temperatures after initial exposure to low but non-freezing temperatures[17]. Cold acclimation is achieved through coordinated expression of a huge battery of cold responsive genes (COR). COR genes encode proteins directly involved in protection against cold damages. Examples are DEHYDRINs[18,19], which protect plants from cold induced dehydration; chaperones, which prevent protein mis-folding; and LATE EMBRYOGENESIS ABUNDANT (LEA) proteins[20,21], which are believed to stabilize membranes and prevent protein aggregation. Because of their robust

inductions in response to cold, CORs were easily identify through differential expression analysis.

Most *COR* genes harbor one to multiple copies of a characteristic *cis*-regulatory sequence in their promoter region, called C-repeat (CRT)/dehydration-responsive element (DRE) repeats. CRT/DRE repeats were found to be necessary for the activation of downstream COR genes and therefore believed to be docking sites for transcription activators[22]. To identify protein components interacting with CRT/DRE, yeast one hybrid was performed. This led to the identification of CRT/DRE BINDING FACTOR 1 (CBF1) as a transcription activator[23]. Constitutive over-expression of *CBF1* leads to the activation of CORs without cold treatment, as well as enhanced tolerance against freezing stress[24]. However, as a result of energy over-consumption, plants over-expressing *CBF3* (homolog of *CBF1*) shows compromised fitness under regular growth conditions[25]. Therefore, expression of CBFs must be tightly controlled.

Through a forward genetic screen for regulatory components of *CBF* expression, *INDUCER OF CBF3 EXPRESSION 1* (*ICE1*) was identified[26]. ICE1 encodes a MYC type transcription factor that is constitutively expressed and further induced after cold treatment. This constitutive expression of *ICE1* provides a system allowing fast activation of CBF3 upon exposure to cold. Mutant *ice1* shows impaired *CBF3* expression and compromised resistance towards freezing stress after cold acclimation[26]. However, surprisingly, *CBF1* or *CBF2* expression is not

obviously affected or even slightly upregulated in the *ice1* mutant. One explanation is that *CBF3* promoter contains more MYC sequences than *CBF1* or *CBF2*. In addition, because *CBF* expressions are also under negative feedback regulation, down-regulation of *CBF3* could lead to the up-regulation of *CBF1* and *CBF2*.

How is ICE1 regulated then? We now know that ICE1 itself is regulated through post-translational modification. HIGH EXPRESSION OF OSMOTICALLY RESPONSIVE GENE 1 (HOS1) was identified to be a RING E3 ubiquitin ligase. Cold triggers the translocation of HOS1 from cytosol to the nucleus where it targets ICE1 for proteasome-mediated degradation[27,28]. Over-expression of *HOS1* leads to the suppression of all the three *CBF*s as well as *COR* genes activated by *CBF*s. Sumoylation of ICE1 has also been reported. It is believed that sumoylation of ICE1 leads to its stabilization by blocking the ubiquitination sites and thereby protected ICE1 from degradation[29].

In summary, CBF pathway is tightly regulated to ensure quick activation of protection against freezing stress and at same time avoids over-consumption of energy when protection is not required.

1.1.4 Temperature entrained circadian clock

Temperature also has an influence on circadian clock in two aspects: entrainment and compensation. Temperature entrainment describes the setting of circadian rhythm based on thermal cycles. *PSEUDORESPONSE REGULATOR 7* and *9* (*PRR7* and *9*) were found to mediate temperature entrainment of circadian

clock[30]. Double mutant of *prr7* and *prr9* displays a temperature dependent elongation of its circadian rhythm. When grown at 22°C/12°C thermal cycle under continuous light, *prr7/prr9* mutant displays a regular 24-hr rhythm. However, this rhythm is lengthened with the increase of temperature. Under 22°C/28°C thermal cycle, *prr7/prr9* mutant displays a 35-hr rhythm while the WT is able to maintain the 24-hr rhythm. This lengthening of rhythm in the double mutant can be explained by the elevation of *CIRCADIAN CLOCK ASSOCIATED 1 (CCA1)* and *LATE ELONGATED HYPOCOTYL (LHY)* expression. Therefore, PRR7 and PRR9 mediate temperature entrainment by controlling *CCA1* and *LHY* expression.

Temperature compensation describes a phenomenon that the circadian clock is able to maintain its robust output across a wide range of temperatures fluctuations. C*CA1 and LHY* expressions are elevated under high temperatures. However, this elevation of CCA1 and LHY expression is very soon suppressed the expression *TIMING OF CAB1 EXPRESSION* (*TOC1*) and *GIGANTEA* (*GI*) which are also induced by high temperatures. In addition, CCA1 is subject to phosphorylation by CASEIN KINASE 2 (CK2)[31], which reduced the transcription activity of CCA1. CK2 activity is also upregulated by high temperatures and thereby it keeps CCA1 activity in check. In summary, although high temperature induces the expression of *CCA1* and *LHY,* counter-balancing forces come into play to diminish the effect of CCA1 and LHY on circadian rhythm and thereby maintain a 24-hr period.

1.1.5 Temperature influence on geographic distribution of plants

Due to the influence of temperature on the growth and development of plants, global warming has affected the geographic distribution as well as diversity of plants. Plant species have been observed to migrate upward to a higher altitude where the temperature is lower[32]. However, certain species already living at the highest altitude have been found to be threatened or extinct[33].

In conclusion, temperature influences almost all aspects of plant lives. Unfavorable temperatures as a consequence of global warming will have detrimental impacts on plants. As described in the previous sections, the downstream temperature responses of plants are well characterized. However, the very initial sensory step remains poorly understood. Intensive studies have been carried out to uncover the mechanisms underlying plant thermal sensing. Although the identities of thermal sensors still remain a mystery, based on the studies in the past decade, we now have better understandings of the early sensory steps.

1.2 Thermal sensory mechanisms in plants

1.2.1 Ca^{2+} dependent thermal sensing

A sequential signaling cascade have been characterized in Ca^{2+}-dependent thermal sensing pathway. It involves membrane fluidity change, $[Ca^{2+}]_i$ increase, activation of Ca^{2+}-sensing proteins and cytoskeleton reorganization.

1.2.1.1 Membrane Fluidity

One of the earliest responses of plants toward temperature change is a change in membrane rigidity. Low temperature increases the rigidity of phospholipid based plasma membrane, while high temperature has the opposite effect. Studies with both Alfalfa (*Medicago sativa*) suspension cells and *Brassica napus* leaves demonstrate that membrane rigidification, triggered by dimethyl sulfoxide (DMSO, a well-known membrane rigidifier) can activate the expression of *COR* genes including *cas30* and *BN115* respectively at room temperature. However, membrane fluidization triggered by benzyl alcohol (BA, a well-known membrane fluidizer) greatly attenuates the cold responses even after prolonged cold acclimation at 4°C[34,35]. Therefore, membrane rigidification is necessary and sufficient for at least part of the cold responses.

1.2.1.2 Cytosolic calcium increase

Ca^{2+}, as a universal second messenger, is involved in almost all aspects of life, including biotic and abiotic stress signaling, regulation of stomatal aperture, circadian regulation, polar tip growth of root hair and pollen tube, and self-incompatibility responses[36]. Because of its role in mediating such a broad spectrum of signaling events, one critical question is how this universal signaling event achieves its specificity.

Ca^{2+} signals take the form of transient increases of cytosolic free Ca^{2+} concentration ($[Ca^{2+}]_i$). It is now known that each Ca^{2+} transient is unique in its

dynamics, or so called Ca^{2+} signatures. Ca^{2+} signatures are composed of three major components: frequency, duration and amplitude. These three components are defined by highly coordinated activities of Ca^{2+} influx into the cytosol through Ca^{2+} channels, as well as efflux out of the cytosol through Ca^{2+} pumps. It is believed that stimulus specific activation and regulation of Ca^{2+} channels as well as pumps define unique Ca^{2+} signatures corresponding to the stimulus. Therefore, Ca^{2+} signatures encode precise information of the nature and intensity of stimuli that trigger them[36].

It has been observed in decades that cold triggers an immediate $[Ca^{2+}]_i$ increase in plants. Electrophysiology studies using *Arabidopsis* mesophyll cells and protoplasts demonstrate that gradual decrease of temperature from 29°C to 16°C triggers a depolarization of plasma membrane from a resting potential of -150mV to -50mV, followed by a recovery up to -100mV and plateaus. Further recovery back to the resting potential requires the return of temperature back to 29°C[37]. Furthermore, this cold induced membrane depolarization is characterized to be an outward rectifying current mediated by calcium permeable non-selective cation channels located on the plasma membrane.

With the identification of calcium sensitive luminescent protein aequorin, *in vivo* real-time quantification of $[Ca^{2+}]_i$ became possible. Using transgenic *Arabidopsis* constitutively over-expressing aequorin, detailed information of cold induced $[Ca^{2+}]_i$ increase in plants has been obtained. It is found that cold induced

$[Ca^{2+}]_i$ increase is not dependent on absolute temperatures, but rather, on the magnitude of temperature difference, as well as the rate of cooling[38]. Upon an instant decrease of temperature from 22°C to 4°C, plants respond by triggering $[Ca^{2+}]_i$ increase in less than one second. Within less than 5 seconds, this cold induced $[Ca^{2+}]_i$ increase is estimated to be from a resting concentration of approximately 0.13μM to a final concentration of approximately 2.2 μM[39-41]. This $[Ca^{2+}]_i$ increase can be significantly attenuated after preincubation with ethylene glycol-bis(β-aminoethyl ether)-N,N,N',N'-tetraacetic acid (EGTA, extracellular calcium chelator) or $LaCl_3$ (plasma membrane calcium channel blocker), indicating that extracellular Ca^{2+} influx across the plasma membrane is a major contribution to cold induced $[Ca^{2+}]_i$ increase[40]. However, EGTA or $LaCl_3$ cannot fully abolish the $[Ca^{2+}]_i$ increase, indicating the presence additional intracellular Ca^{2+} sources. With the help of chimeric aequorin targeted to vacuoles, vacuolar Ca^{2+} efflux has also been detected in response to cold[40]. However, whether this vacuolar Ca^{2+} efflux is directly triggered by cold, or indirectly by cold induced extracellular Ca^{2+} influx remains unknown.

Despite the well recognition cold induced $[Ca^{2+}]_i$ increases, the molecular identities of the corresponding Ca^{2+} channels remain elusive. Several proteins have been suggested to be temperature activated calcium channels in plants, including cyclic nucleotide gated calcium channels (CNGCs)[42]. *cngc* loss of function mutants in *Physcometrilla patens* (*cngcb*) and in *Arabidopsis thaliana*

(*cngc2*) both display hypersensitivity in heat induced membrane depolarization as well as constitutive expression of heat shock proteins. Consequently, these mutant plants are more resistant to heat stress. However, probably because of the energy over-consumption in maintaining constitutive protection against heat stress, both *Physcometrilla* and *Arabidopsis* mutants display obvious growth defects under regular growth conditions. Later, the same group found that *cngcb* and *cngcd* double mutant in *Physcometrilla* triggers heat induced $[Ca^{2+}]_i$ increase at a lower temperature compare to the wild type (WT), indicating a sensitized response towards heat stress in the absence of CNGCb and CNGCd[43]. Therefore, CNGCs are suggested to be negative mediators of heat induced $[Ca^{2+}]_i$ increase in plants. However, direct evidence showing that CNGCs themselves form heat activated Ca^{2+} channels is lacking. Whether the hypersensitive Ca^{2+} response is a direct consequence of defective heat sensing is unclear either.

More and more evidences suggest the presence of thermal. However, the identities of these sensors remain elusive. In addition, while $[Ca^{2+}]_i$ increase is faithfully observed in response to temperature changes, direct genetic evidence proving that this $[Ca^{2+}]_i$ increase play a role in mediating thermal perception is missing.

1.2.1.3 Ca^{2+} sensing proteins

Ca^{2+} sensing proteins are able to interact with cytosolic Ca^{2+}, decode information in form of Ca^{2+} signatures, and subsequently pass the information onto

the downstream components. Plants possess a large repertoire of Ca^{2+} sensing proteins, including CDPKs (Ca^{2+}-DEPENDENT PROTEIN KINASEs), CaMs (CALMODULINs), CBLs (CALCINURIN B LIKE PROTEINs), etc.[3] They act as positive or negative regulators in Ca^{2+} dependent signaling events[44-47]. Ca^{2+} sensing proteins are classified into two categories: sensor relay proteins and sensor responder proteins. Sensor relay proteins carry Ca^{2+} binding domains as well as effector domains. Therefore, they have integrated functions of decoding Ca^{2+} signatures and activating the downstream signaling events accordingly. In contrast, sensor relay proteins lack the effector domain and therefore, need interaction with their target proteins to activate the downstream signaling events.

1.2.1.4 Cytoskeleton reorganization

Cytoskeleton functions as a continuous mechanical coupling network underneath the plasma membrane. It modulates environmental perception and subsequently transmit the signal to the downstream responses[48]. Studies using *Nicotiana plumbaginifolia* protoplast demonstrate that disruption of microtubules by colchicine or oryzalin leads to magnified increases of $[Ca^{2+}]_i$ upon cold shock. The magnitude of cold induced $[Ca^{2+}]_i$ increase is correlated to the degree of microtubule disruption. On the other hand, disruption of microfilament has little effect on cold induced $[Ca^{2+}]_i$ increase. However, a synergistic effect was observed when microtubules and microfilaments are disrupted simultaneously[49]. The same phenomenon has been observed in alfalfa suspension cells as well as in *Brassica*

napus leaves[34,35], demonstrating a highly conserved role of cytoskeleton reorganization in mediating thermal perception.

It is not clear whether this cytoskeleton disruption directly opens cold activated calcium channels through mechanical force or indirectly through other mechanisms. However, considering that cytoskeleton reorganization occurs much slower than $[Ca^{2+}]_i$ increase after cold treatment[40,50], it is unlikely that cytoskeleton reorganization is required to initiate cold induced $[Ca^{2+}]_i$ increase. The more plausible possibility is that cytoskeleton disruption modulates the physical properties of the plasma membrane and thereby sensitizes calcium channels, leading to a magnified cold induced $[Ca^{2+}]_i$ increase.

1.2.2 Calcium independent thermal sensing

1.2.2.1 Chromatin mediated thermal sensing

Thermal perception has been suggested to occur at epigenetic level. One of the best known example is warm temperature perception mediated by alternative histone H2A.Z[51].

Through a forward genetic screen of mutants constitutively over-expression of *HEAT SHOCK PROTEIN 70* (*HSP70*), two allelic mutations of *ARP6* were identified. Both *arp6* mutants constitutively express warm temperature transcriptome in addition to *HSP70,* and therefore phenocopy warm grown plants at cool temperatures. ARP6 encodes a subunit of SWI1 complex, which is highly conserved in eukaryotes. SWI1 complex functions to insert alternative histone

H2A.Z into nucleosome in replace of H2A. This replacement occurs at the +1 site of the promoter region, which is believed to be a check point for RNA polymerase II. High occupancy of H2A.Z at +1 site functions as a hurdle for RNA polymerase II and thereby suppress the expression of the downstream gene. Temperature dependent incorporation of H2A.Z into nucleosomes has been demonstrated using ChIP assay. As expected, the interaction between H2A.Z and DNA is promoted at low temperature and diminished at high temperature. Therefore, at high temperature, RNA polymerase II will be more accessible to its target promoters and activate gene expression.

Therefore, alternative histone H2A.Z is proposed to be an essential mediator that perceives warm temperature in *Arabidopsis*. However, through ChIP assay, it cannot be fully excluded that alternative histone H2A.Z itself does not sense temperature changes, but rather, an unknown component upstream does and subsequently relay the signal onto H2A.Z by protein modification, leading to a higher affinity of H2A.Z to DNA. Therefore, the possibility that temperature dependent, alternative histone mediated chromatin modification might also be downstream of calcium signaling cannot be fully ruled out.

1.2.2.2 Phytochrome mediated perception

Phytochrome B (PhyB) is recently suggested to be a temperature sensor in plants[52,53]. PhyB is a dimeric photoreceptor protein that plays an important role in regulating plant growth and development. PhyB exists in two interconvertible

forms. Functionally active form (Pfr) absorbs far red light and will thus be converted to the inactive form (Pr). Inactive Pr absorbs red light and will be converted back to active Pfr. This interconversion is accompanied by a subcellular translocation. Pfr is located in the nucleus as nuclear bodies, where it associates with DNA and exerts its transcription regulator function; while Pr is excluded from the nucleus and is located in the cytosol[54]. It is now known that in addition to far red absorption, Pfr can also return to Pr spontaneously through a process called thermal relaxation. Thermal relaxation can be accelerated at high temperature, indicating a temperature dependent regulation of PhyB. In line with this observation, PhyB nuclear bodies decrease in size with the increase of temperature[52]. Furthermore, DNA binding ability of PhyB also decreases at high temperature[53]. Genetically, *phyb* loss of function mutant grown at 17°C phenocopies plants grown at warm temperatures. Consistent with this observation, plants expressing constitutively active form of PhyB failed to develop high temperature mediated morphogenesis at 27°C. Therefore, the function of PhyB is to suppress warm temperature responses at cool temperatures. Or in other words, PhyB de-represses warm temperature responses with the increase of temperature.

In summary, intensive studies have been carried out to understand how plants sense and respond to temperature changes. These studies contribute to a more complete picture of temperature responses in plants, including molecular mechanisms underlying vernalization, acclimation and thermomorphogenesis.

However, although there has been continuous progress in understanding thermal sensing, the direct molecular components, especially in temperature induced $[Ca^{2+}]_i$ increase, remain unidentified. However, a lot has been known regarding thermal sensing in other species, which may help us better understand thermal sensing in plants.

1.3 Thermal sensing across species

Temperature varies spatially and temporally[55]. This variation has drastic influence on cellular, metabolic homeostasis and consequently, survival of a species. Therefore, the ability to precisely and quickly perceive temperature changes in the environment is fundamental for the fitness and survival of a species[56].

1.3.1 Thermal sensing in microorganisms

Temperature perception in microorganisms has been proposed at different cellular levels. DNA and RNA conformations are found to be influenced by temperature changes and this is suggested to be a potential perception mechanism by modulating the efficiency of transcription and translation[56]. Membrane fluidity has also been suggested to be a thermometer. In *B. subtilis*. Low temperature is known to trigger a rigidification of membrane lipid. This membrane rigification will be perceived by protein kinase DesK. DesK consists of four transmembrane domains and a cytosolic kinase domain. It is suggested that

the transmembrane domains of DesK detect the lipid fluidity in response to temperature change and thereby modulates its cytosolic domain. Membrane rigidification favors the kinase activity of the cytosolic domain, which phosphorylates its interacting partner DesR[57,58]. Phosphorylated DesR dimerizes and activates the transcription of fatty acid desaturases, which introduce double bonds into the fatty acid chains in the plasma membrane and thereby increase membrane fluidity. Thus, DesK mediates lipid desaturation in response to cold induced membrane regidification and thereby protects membranes from freezing damage.

Similar system is adopted in cyanobacterium *Synechocystis* sp. PCC6803. In *Synechocystis*, Hik33 is proposed to be the membrane embedded thermometer. Hik33 autophosphorylation occurs upon low temperature induced membrane rigidification. Subsequently, Hik33 transfer this phosphate group via Hik19 onto Rer1. Rer1 in turn activates the transcription of fatty acid desaturase genes, leading to the desaturation of membrane lipids[59,60].

Therefore, thermal sensing through detection of membrane fluidity change seems to be widely adopted in micro-organisms.

1.3.2 Thermal sensing in nematode

Despite the simplicity of their nervous system, *C. elegans* display a complex behavior towards temperature changes[56]. For example, when placed on a thermal gradient, *C. elegans* display a preference for their cultivation temperature[61]. Even

more interestingly, when food deprivation was given at a certain temperature, *C. elegans* develop a learning and memory behavior such that they avoid the particular temperature associated with starvation[62].

Remarkably, a single sensory neuron called AFD is sufficient for the temperature detection. When AFD is ablated with laser microbeams, the thermal - taxing behavior towards the cultivation temperature is abolished[63]. Subsequently, Kimura *et. al.* demonstrated that AFD neuron responds to relative temperature change instead of absolute temperature by a transient $[Ca^{2+}]_i$ increase[64]. Genetic studies show mutation in both *tax-2* and *tax-4* affects the thermotactic behavior of *C. elegans*.[64,65]. *tax-4* and *tax-2* genes encode α- and β-subunits respectively of a cGMP gated ion channel. Functional studies in HEK293 cells as a heterologous system, showed that TAX-4 alone can form functional channels as homotetramers, while TAX-2 alone is not functional. When TAX-2 and TAX-4 are co-expressed, functional channels can also be formed as heterotetramers[65,66]. In line with this observation, temperature induced $[Ca^{2+}]_i$ increase is totally abolished in *tax-4* null mutants and expression of *Tax-4* alone can rescue the phenotype in tax-2/tax-4 double mutant[64]. Therefore, *Tax-4* is the primary functional unit mediating temperature induced $[Ca^{2+}]_i$ increase in AFD neuron.

To further elucidate the molecular mechanism that translates the temperature change to the signal of cGMP which subsequently activate cGMP-gated ion channels, reverse genetic studies were performed. It is found that among

all the guanylyl cyclase genes in *C. elegans* genome, *gcy-8*, *gcy-18* and *gcy-23* are exclusively expressed in AFD and are localized at the nerve endings[67]. Double or triple mutants display defects in thermotactic behavior in *C. elegans* which is similar to the phenotype of *tax-4* mutant. However, single mutant of any of the three genes does not cause any abnormality in the worms, indicating a high functional redundancy among them. Thus, GCY-8, -18 and -23 are suggested to the thermal sensors in C. elegans that produce cGMP and thereby trigger temperature induced $[Ca^{2+}]_i$ increase in AFD neurons.

1.3.3 Thermal sensing in fruit fly

Like *C. elegans*, *Drosophila* at both larval and adult stages also display a preference for a certain temeprature[68]. While adult flies prefer 24°C, *Drosophila* larva favor 18°C regardless of their cultivation temperature. Through a forward genetic screen, Tracey *et. al.*, identified a mutant *painless*, which displayed drastically compromised response towards high temperature ranging from 42°C to 48°C[69]. *Painless* encode a protein in Transient Receptor Potential (TRP) A subfamily expressed in a subset of multidendritic neurons. Suction electrode recordings show that multidendritic neurons display heat evoked calcium spikes, which is absent in *painless*. However, response towards temperature above 52°C is not affected in *painless*, indicating the presence of multiple sensors activated at different temperature ranges. In addition to *PAINLESS, Drosophila* possess three

more TRPA proteins, named as *dTRPA1, dTRPA2* and *dTRPA3*[70]. dTRPA1 is responsive to temperatures above 27°C when expressed in heterologous systems[71]. Larva with *dTRPA1* knocked down by RNAi failed to display thermotaxis towards their optimum temperature[72]. dTRPA2, or alternatively PYREXIA, responds to temperature above 40°C by evoking an ionic current[73]. *dtrpa2* null mutant displays strong paralytic behavior at temperatures higher than 40°C. In addition to TRP channels, proteins involved in histamine signaling have been suggested to mediate temperature sensing in *Drosophila*, including a histamine gated ion channel[74]. However, the identity of sensors responsible for low temperature sensing are yet to be identified.

Therefore, thermal sensing in *Drosophila* involves multiple signaling pathways gated by different thermal sensitive proteins.

1.3.4 Thermal sensing in vertebrates

Vertebrate thermal sensors are identified largely due to the recognition that certain plant extracts trigger similar psychological sensations of hot and cold. Through an expression cloning strategy based on Ca^{2+} influx in response to capsaicin, Caterina *et. al.*, identified TRPV1 as a capsaicin sensitive Ca^{2+} permeable channel[75]. In addition to capsaicin, TRPV1 is also activated by noxious heat at around 42°C[75] and proton when expressed in heterologous systems[76]. Therefore, TRPV1 null mice display reduced responsiveness to temperatures

above 50°C. In addition, inflammation caused hyperalgesia is known to be mediated by local acidosis of injured tissues and TRPV1 null mice fail to develop hyperalgesia in response to thermal stimuli after inflammatory tissue injury[77]. Thus, TRPV1 is suggested to be a polymodal Ca^{2+} permeable channel that integrates multiple stimuli related to pain sensation[77].

Later using similar expression screen strategy, TRPM8 was identified as a Ca^{2+} permeable cold and menthol activated channel[78,79]. TRPM8 is responsive at temperature below 26°C and evokes a stronger current at 8°C, and therefore, may mediate sensing of both innocuous cool and noxious cold temperatures.

Since then, the significance of TRP channels in vertebrate thermosensation has been recognized and more TRPs are identified to be thermosensors responsive to different temperature ranges. For example, TRPV2 is found to mediates sensing of noxious heat at above 52°C[80]; TRPV3 mediates sensing of temperature of 22°C to 40°C; TRPV4 is triggered at above 25°C[81]; and TRPA1 may respond to cold temperatures below 10°C[82]. Therefore, vertebrates developed an array of TRP channels to detect a broad spectrum of physiologically meaningful temperatures.

Interestingly, some animals have developed creative modifications on TRP channels for additional purposes. For example, vampire bat employed alternative splicing of TRPV1 specifically in their infrared sensing pit organ and thus decreased the activation temperature from 42°C to 30°C. Therefore, this TRPV1

splicing variant enables vampire bat, as an obligatory blood-feeding animal to locate warm blood animals by infrared sensing[83]. Pit-baring snakes are also able to detect infrared radiation. Different from vampire bats, pit-baring snakes evolved an orthologue of mouse TRPA1 which allows high sensitivity infrared detection[84].

In summary, TRP channels play a fundamental role in temperature sensing and are highly conserved among vertebrates.

1.4 Hunting thermal sensors in plants

Based on the knowledge of thermal sensing in different species, it is found that some of the functional mechanisms are well conserved throughout evolution, for instance, membrane fluidity change and $[Ca^{2+}]_i$ increase. However, different organisms employ different molecular components in the signaling pathways. For example, micro-organisms adopted two component system, *C. elegans* adopted CNGC mediated $[Ca^{2+}]_i$ increase while *Drosophila* and vertebrates adopted TRP channels to sense and trigger temperature induced $[Ca^{2+}]_i$ increase.

As expected, although membrane fluidity change and $[Ca^{2+}]_i$ increase have both been reported in plants in response to temperature changes, no orthologue of any known thermal sensors has been identified in plants. Therefore, plants might have also adopted unique molecular components for thermal sensing. One promising strategy to identify thermosensors in plants is unbiased forward genetic screen.

Chapter 2 Ca^{2+}-imaging based genetic screen for plant thermal sensors

2.1. Introduction

Intensive genetic screens of temperature sensitive mutants have been carried out. For instance, the expression of *COR* gene *RD29A* was used as a marker to screen for mutants insensitive to cold, leading to the identification of *HOS1*[85]. However, the molecular identities of thermal sensors still remain a mystery. One possible reason is that these markers used in early genetic screens were downstream in the signaling pathways. An upstream genetic marker which directly reflects the activity of thermal sensors would thus provide the advantage of a narrow screening spectrum. This narrow screening spectrum will maximize the resolution of the genetic screen for thermal sensors.

One earliest response of plants towards low temperatures is a drastic increase of $[Ca^{2+}]_i$[40]. This $[Ca^{2+}]_i$ increase occurs almost immediately after cold shock, directly reflecting the activity of cold activated calcium channels. Tools for high throughput measurements of $[Ca^{2+}]_i$ are also available. Transgenic *Arabidopsis* constitutively over expressing aequorin have been generated[39-41]. Aequorin is a calcium sensitive photoprotein isolated from *Aequorea victoria*. It consists of a polypeptide apoaquorin and a luminophore, coelenterazine. At the presence of calcium ions, aequorin undergoes a conformational change, and converts coelenterazine to exicted coelenteramide and CO_2. Excited

coelenteramide will subsequently return to its ground state, during which energy is dissipated as blue light[86]. The intensity of blue light can be readily monitored with a CCD camera, making high throughput genetic screen feasible. It is noteworthy that genetic screen using aequorin based Ca^{2+} imaging has led to the identification of osmolarity sensitive Ca^{2+} channel, *HYPEROSMOLARITY INDUCED* $[Ca^{2+}]_i$ *INCREASE 1* (*OSCA1*) in *Arabidopsis*[87].

Therefore, to identify thermal sensors in *Arabidopsis*, we decided to adopt aequorin-based calcium imaging and screen for mutants with compromised cold induced $[Ca^{2+}]_i$ increase.

2.2. Results

2.2.1 Ca^{2+}-imaging based genetic screen for mutants with defects in cold induced $[Ca^{2+}]_i$ increase

M2 generation of ethyl methanesulfonate (EMS) mutagenized *Arabidopsis* seedlings were screened individually for the phenotype of compromised cold induced $[Ca^{2+}]_i$ increase. A total of over 100,000 M2 plants were covered in this genetic screen. Approximately 10% seedlings displayed compromised cold induced $[Ca^{2+}]_i$ increase in the initial screen and all these ~10,000 seedlings were transferred to soil for M3 seeds (Figure 1). In M3 generation, pooled progenies of each M2 candidate were analyzed to check if the mutant phenotype is genetically heritable. In addition, the functionality of aequorin system was examined to ensure that the mutant phenotype is not caused by a mal-functional aequorin based Ca^{2+}

detecting system. M3 seedlings maintaining mutant phenotype towards cold while possessing a well functional aequorin based calcium sensing system were kept and M4 were collected.

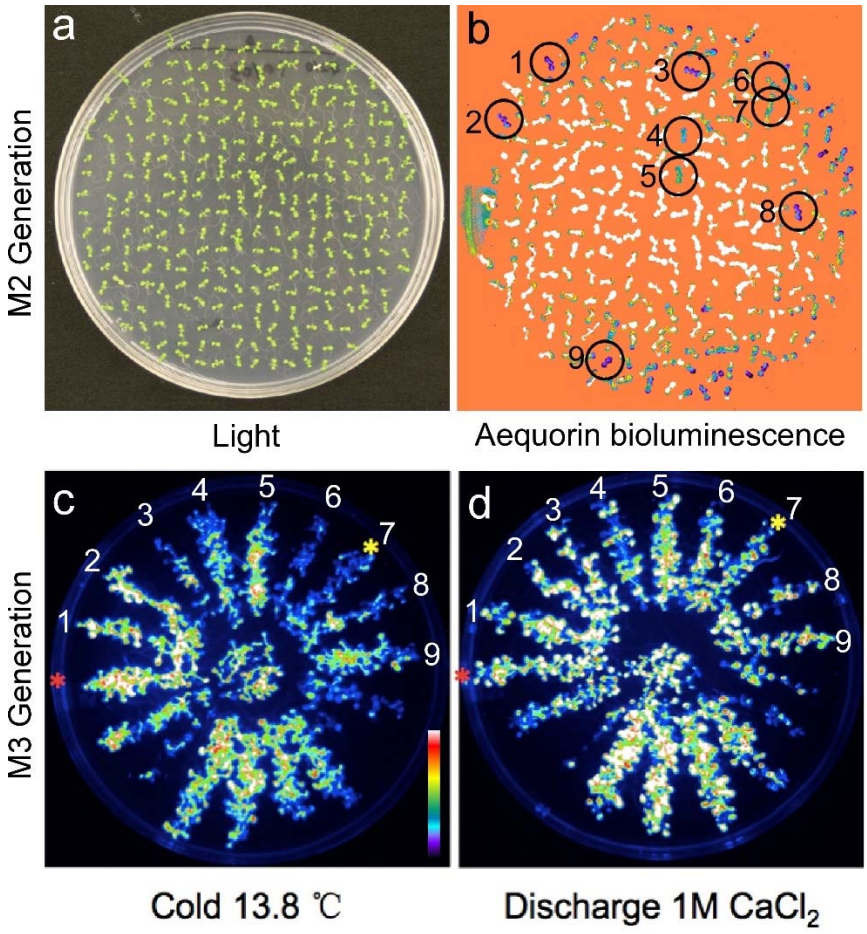

Figure 1 Genetic screen of mutants with compromised cold induced $[Ca^{2+}]_i$ increases

a, Light image of eight-day-old seedlings in the initial screen (M2). **b,** Bioluminescence image of cold induced $[Ca^{2+}]_i$ increase in individual seedlings (M2). Dark circles, candidate mutants. **c,** Bioluminescence image of pooled M3 seedlings corresponding to each M2 candidate mutant. red asterisk, WT; yellow asterisk, candidate mutant. **d,** Total aequorin bioluminescence measured by treating c with 1M $CaCl_2$. ($[Ca^{2+}]_i$ was scaled by a pseudo-color bar.)

An additional round of confirmation was performed using pooled M4 seedlings. Three M4 lines were examined for each mutant. As a result, approximately 40 candidate mutants displayed compromised cold induced $[Ca^{2+}]_i$ increase (*coca*). Results of *coca1, coca2, coca3* and *coca4* are shown as representatives (Figure 2).

All of the three *coca4* lines are fully responsive to low temperature, meaning that the mutant phenotype observed in M2 and M3 generation is not stably inherited in the M4 generation. *coca1, coca2* and *coca3* are able to stably maintain the *coca* phenotype in the M4 generation.

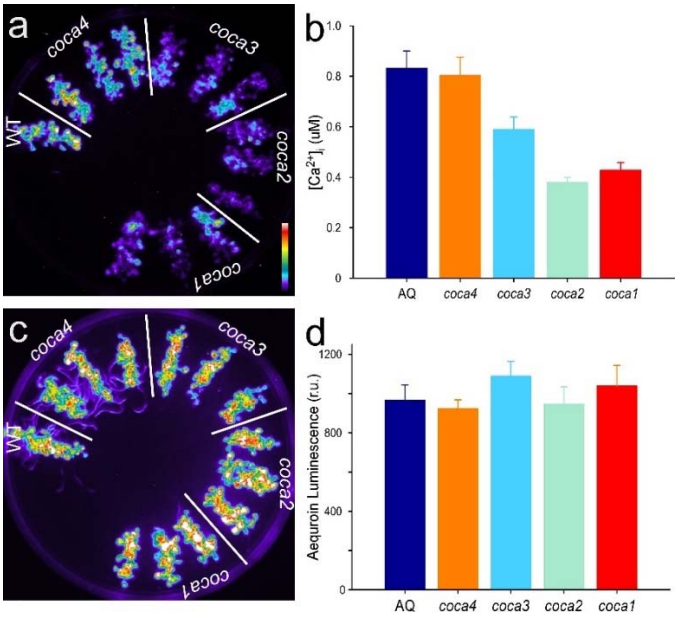

Figure 2 Cold induced $[Ca^{2+}]_i$ increase in *coca* candidates.
a, Bioluminescence image of cold induced $[Ca^{2+}]_i$ increase (M4). **b,** Quantification of cold induced $[Ca^{2+}]_i$ increase in a. **c,** Total aequorin bioluminescence recorded after 1M $CaCl_2$ treatment. **d,** Arbitrary quantification of total aequorin bioluminescence recorded in c. ($[Ca^{2+}]_i$ was scaled by a pseudo-color bar. mean ± standard error of mean (s.e.m.), n = 30)

Based on the assumption that thermal sensors should be able to differentiate stimuli and therefore displaying certain level of specificity, responses of the 40 *coca* candidates towards other stimuli were examined and only *coca1, 2, 3* and *4* are shown here (Figure 3). We found that *coca2* and *coca3* are insensitive to cold but fully responsive to H_2O_2. However, both *coca3* and *coca2* display compromised $[Ca^{2+}]_i$ increase in response to sorbitol, $CaCl_2$ and NaCl, indicating a defect in sensing osmotic as well as ionic stimuli. *coca1* shows defects only in low temperature sensing, and is fully responsive towards all the other stimuli tested across the concentration range.

Therefore, *coca1*, *coca2* and coca3 were chosen for further analysis and physical mapping. Only *coca1* and *coca2* will be described in this dissertation.

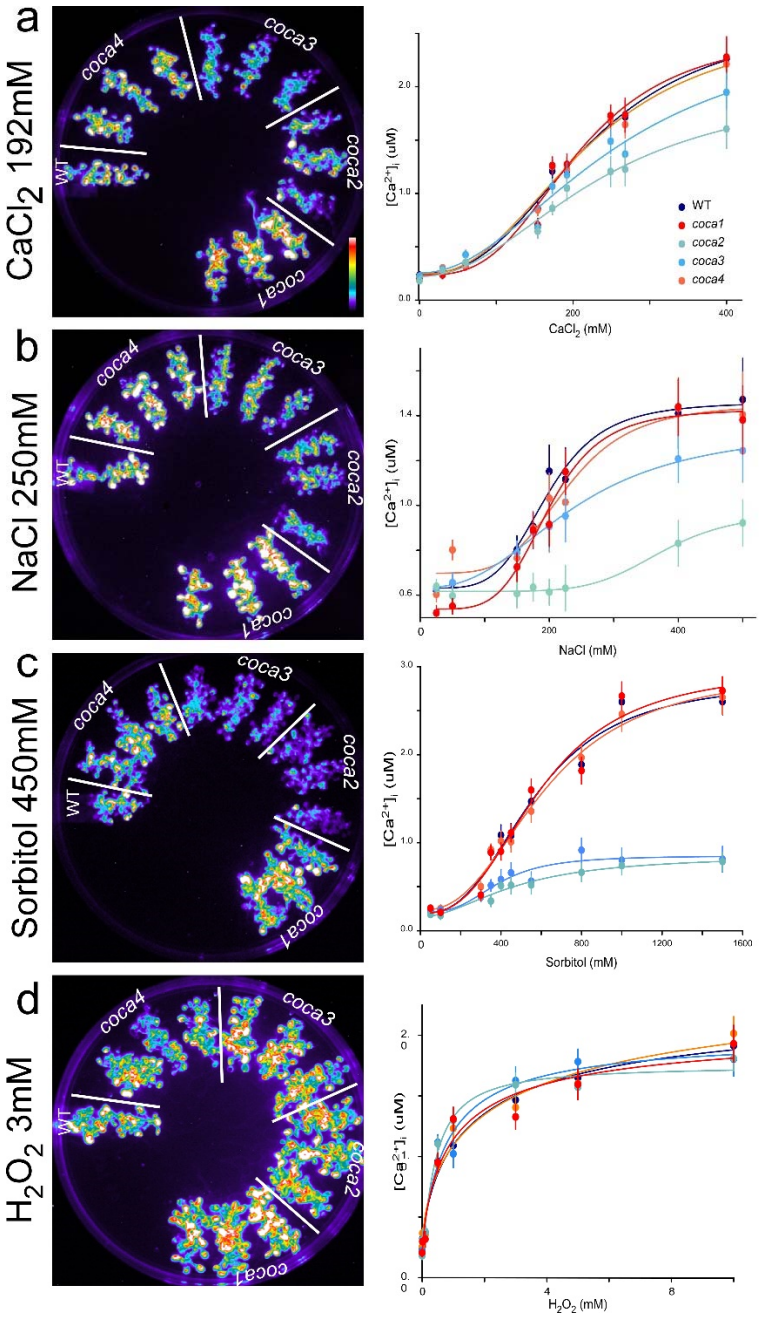

Figure 3 $[Ca^{2+}]_i$ increase in response to ionic, osmotic and oxidative stimuli. Bioluminescence images and corresponding quantifications of $[Ca^{2+}]_i$ increases triggered by **a,** $CaCl_2$ **b,** NaCl **c,** Sorbitol and **d,** H_2O_2. Bioluminescence was recorded for 5 min in each treatment. ($[Ca^{2+}]_i$ was scaled by a pseudo-color bar. mean ± s.e.m.; n=30).

2.2.2 coca1 *is specifically defective in ambient cool temperature induced* $[Ca^{2+}]_i$ *increase*

2.2.2.1 Aequorin based calcium imaging of low temperature induced $[Ca^{2+}]_i$ *increase in* coca1

coca1 does not display any observable morphological or physiological difference compare to the WT under regular growth conditions. Basal Ca^{2+} concentration in *coca1* is similar to that in the WT. However, upon an instant decrease of temperature from 22°C to 14°C as cold treatment, *coca1* displayed significantly compromised $[Ca^{2+}]_i$ increase compare to the WT. After quantification[40,87], we found that cold triggers an increase of $[Ca^{2+}]_i$ in WT up to approximately 0.8μM, while $[Ca^{2+}]_i$ in *coca1* failed to exceed 0.4μM. To test if this compromised $[Ca^{2+}]_i$ increase is caused by a less efficient aequorin based calcium detecting system in the *coca1*, the remaining aequorin bioluminescence after cold treatment was quantified by treating seedlings with 1M $CaCl_2$ solution supplemented with 10% ethanol. We found that *coca1* possess the same amount of total aequorin bioluminescence compare to the WT.

Therefore, *coca1* is a mutant with impaired cold induced $[Ca^{2+}]_i$ increase (Figure 4).

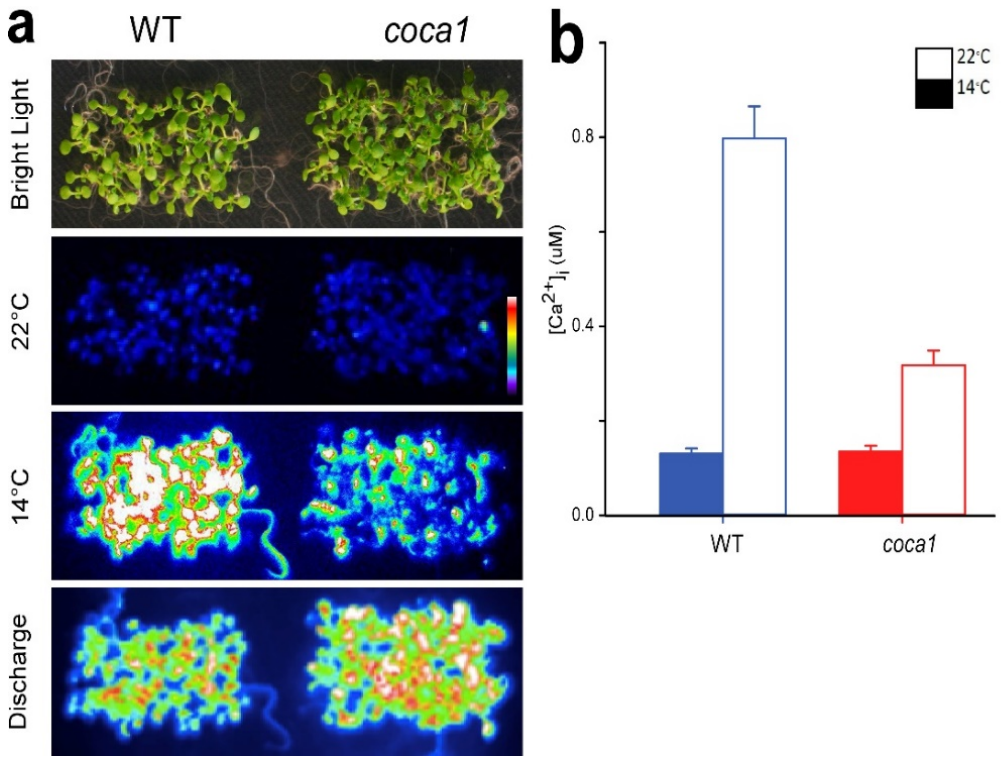

Figure 4 Identification of *coca1* mutant with compromised cold induced $[Ca^{2+}]_i$ increase in *Arabidopsis*.
a, Cold induced $[Ca^{2+}]_i$ increase in WT and in *coca1* mutant. Seedlings were treated with 22°C or 14°C water and aequorin bioluminescence was recorded. **b,** Quantification of cold induced $[Ca^{2+}]_i$ increase in leaves from a. Data from three independent experiments are shown ($[Ca^{2+}]_i$ was scaled by a pseudo-color bar. mean ± s.e.m.; n=30).

To understand the dynamics of cold induced $[Ca^{2+}]_i$ increase in *coca1*, time-course analysis was performed (Figure 5). Both WT and *coca1* respond to low temperature with a single wave of calcium transient. *coca1* responds at approximately the same time compare to the WT and the whole calcium transient lasts for approximately the same duration. However, the peak calcium concentration is more than two folds lower in *coca1* compare to the WT.

Therefore, *coca1* does not alter the frequency or duration of cold induced $[Ca^{2+}]_i$ increases. But rather, the compromised $[Ca^{2+}]_i$ increase is a result of attenuated magnitude in *coca1*.

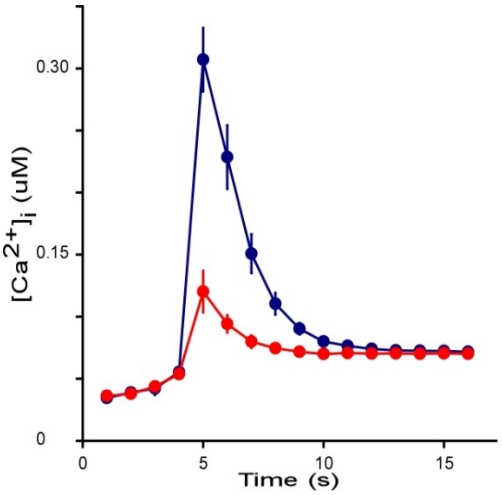

Figure 5 Time course analysis of cold induced $[Ca^{2+}]_i$ increase in *coca1*
Seedlings were treated with 14°C water and luminescent signal was recorded every other second for a duration of one second. Data from two independent experiments are shown (mean ± s.e.m.; n=20).

Next, responses of *coca1* towards different temperatures were examined (Figure 6). A Hill curve can be fitted to the data with an apparent dissociation constant (K_d) of 12.4°C for the WT and 8.8°C for *coca1*. Hill coefficient is 5.6 for the WT and 3.9 for *coca1*. Interestingly, there is no obvious difference between coca1 and WT at 6°C or 22°C. Q_{10} for the log phase is 0.25 for WT and 0.1 for *coca1*.

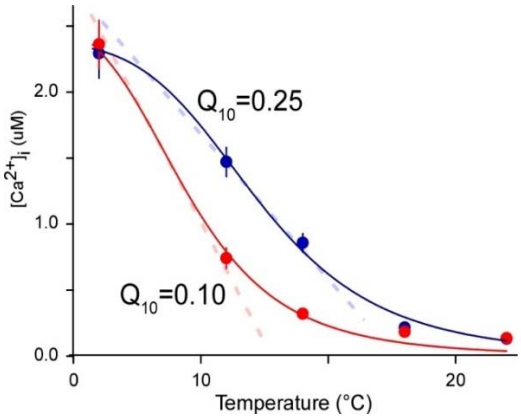

Figure 6 Increase of $[Ca^{2+}]_i$ in *coca1* as a function of temperature gradient.
$[Ca^{2+}]_i$ was quantified from 6°C to 22°C. Bioluminescence was recorded for 3 min. Data from two independent experiments are shown (mean ± s.e.m.; n=30).

2.2.2.2 Cameleon based calcium imaging of cold induced $[Ca^{2+}]_i$ increase in coca1.

We further characterized cold induced $[Ca^{2+}]_i$ increase using a parallel system Yellow Cameleon 3.6 (YC3.6)[88-90]. Similar to aequorin, YC3.6 is a calcium sensitive protein. Unlike aequorin, YC3.6 is based on fluorescence resonance energy transfer (FRET). It is a chimeric protein consists of cyan fluorescent protein

(CFP), CaM, M13 peptide and yellow fluorescent protein (YFP). Binding of Ca^{2+} with CaM facilitates the interaction between CaM and M13 and leads to a conformational change which subsequently brings CFP and YFP to close proximity and thus increases the efficiency of FRET between CFP and YFP[91].

There are two main purposes of characterizing cold induced $[Ca^{2+}]_i$ increase using YC3.6. First, we would like to confirm the *coca* phenotype in a different system. Second, YC3.6 provides a higher resolution of Ca^{2+} dynamics at tissue and cell level compare to aequroin.

Consistent with the observations in leaves with aequorin imaging, *coca1* displayed a compromised cold induced $[Ca^{2+}]_i$ increase in root elongation zone using YC3.6 imaging (Reduced cold induced [Ca2+]$_i$ increase in *coca1* root. **a,**). However, the difference of cold induced $[Ca^{2+}]_i$ increase between WT and *coca1* in root is less prominent compare to that in leaves.

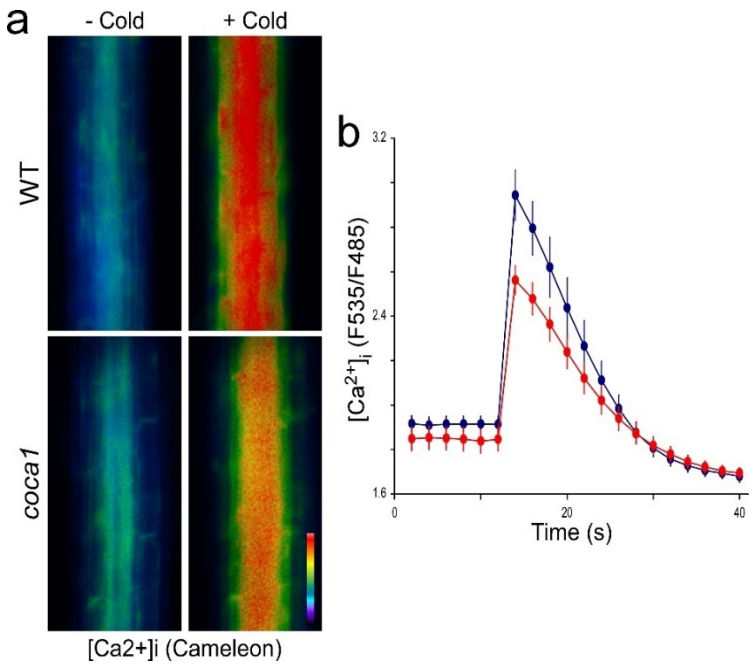

Figure 7 Cold induced $[Ca^{2+}]_i$ increase in *coca1* in Arabidopsis root.
Reduced cold induced $[Ca^{2+}]_i$ increase in *coca1* root. **a,** FRET imaging of cold induced $[Ca^{2+}]_i$ increase was carried out in root. Emission images (F535 and F485) of roots were taken every 2 s, and ratiometric images before cold were shown. F535:F485 ratio is scaled by a pseudo-colour bar. **b,** Relative quantification of a.

2.2.2.3 coca1 displays lower fitness at low temperature

coca1 does not show any significant growth and development difference compare to the WT under regular growth conditions. However, when grown at low temperature on Ca^{2+} deficient medium, they displayed shorter roots compare to the WT (Figure 8), indicating a decreased fitness at low temperature.

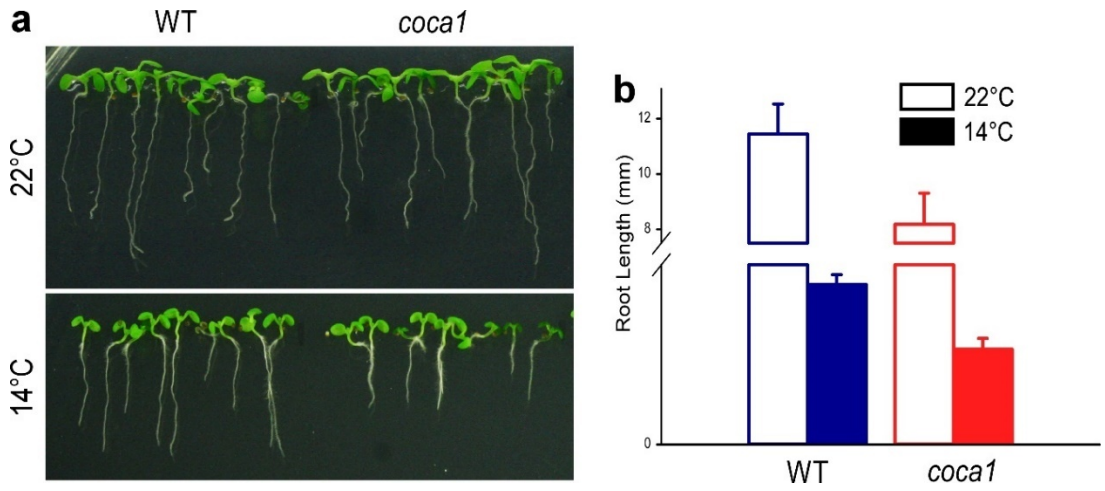

Figure 8 *coca1* shows lower fitness at low temperatures.
a, Seedlings were grown at 22°C or 14°C for 3 weeks. **b,** Quantification of the root length as shown in a. (mean ± s.e.m., n=90)

2.2.3 coca2 *is a mutant defective in cold induced* $[Ca^{2+}]_i$ *increase*

coca2 is identified as another mutant with compromised cold induced $[Ca^{2+}]_i$ increases. There is no observable growth and development difference between *coca2* and WT and the resting $[Ca^{2+}]_i$ in *coca2* is the same as that in the WT. *coca2* displays approximately half $[Ca^{2+}]_i$ increases compare to WT in response to cold (Figure 9). Time course analysis showed that *coca2* retains the same frequency and duration of cold triggered Ca^{2+} signature. However, the magnitude is greatly compromised compare to the WT (Figure 10). *coca2* showed slightly lower cold induced $[Ca^{2+}]_i$ increase at temperature below 6°C, meaning that *coca2* is insensitive to not only ambient cool temperature but also to cold temperatures (Figure 11).

Therefore, we conclude that *coca2* is a mutant with defects towards broader temperature range, as well as osmotic and ionic stimuli.

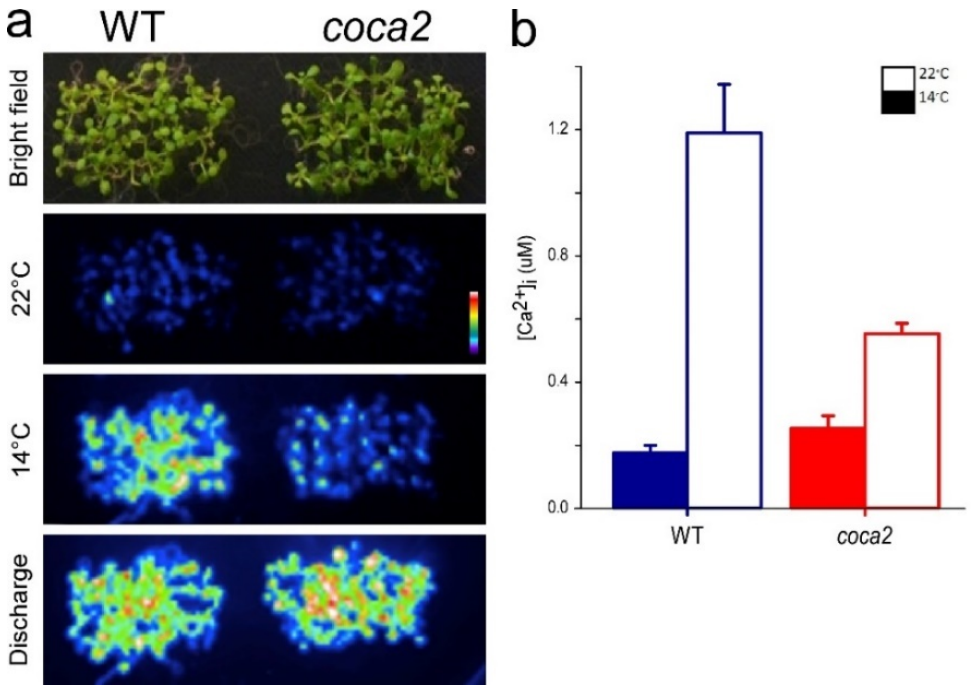

Figure 9 Identification of *coca2* mutant with compromised cold induced $[Ca^{2+}]_i$ increase in *Arabidopsis*.
a, Cold induced $[Ca^{2+}]_i$ increase in WT and in *coca1* mutant. Seedlings were treated with 22°C or 14°C water and aequorin bioluminescence was recorded. **b,** Quantification of cold induced $[Ca^{2+}]_i$ increase in leaves from a. Data from three independent experiments are shown ($[Ca^{2+}]_i$ was scaled by a pseudo-color bar. error bar = mean ± s.e.m.; n=30).

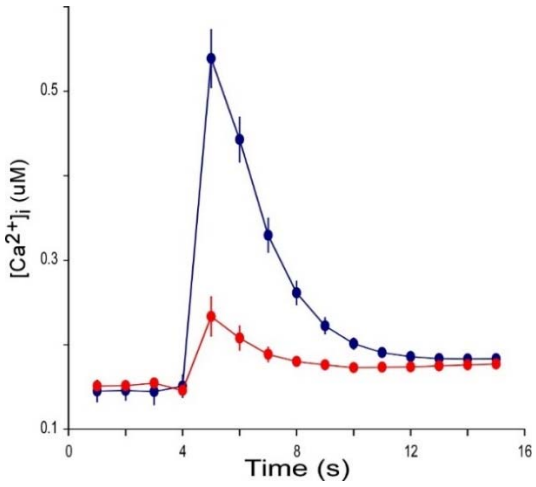

Figure 10 Time course analysis of cold induced $[Ca^{2+}]_i$ increase in *coca2*

Seedlings were treated with 14°C water and luminescent signal was recorded every other second for a duration of one second. Data from two independent experiments are shown (error bar = mean ± s.e.m.; n=20).

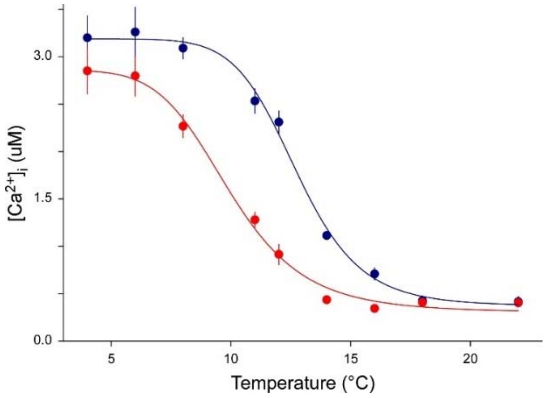

Figure 11 Increase of $[Ca^{2+}]_i$ in *coca2* as a function of temperature gradient.

$[Ca^{2+}]_i$ was quantified from 4°C to 22°C. Bioluminescence was recorded for 3 min. Data from two independent experiments are shown (error bar = mean ± s.e.m.; n=30).

2.3 Discussion

Temperature, as one of the most influential environmental factors, shapes the physiology and survival of plants. Therefore, intensive studies have been carried out to unveil the mechanisms of plant thermal perception and responses. To date, the downstream thermal responses are well understood. However, despite intensive efforts, the upstream thermal perception remain poorly understood. Therefore, we decided to take the advantage of aequorin based calcium imaging and hunt for thermal sensors in *Arabidopsis thaliana*.

Through this forward genetic screen, we identified several mutants defective in cold induced $[Ca^{2+}]_i$ increase. *coca1* and *coca2* were described.

coca1 displays a drastically compromised $[Ca^{2+}]_i$ increase upon instant exposure to ambient cool temperatures. Analysis of the dynamics of this cold induced $[Ca^{2+}]_i$ increase reveals that the frequency and duration of the calcium signature is not affected. However, the magnitude of the transient is decreased by more than two folds. Characterization of *coca1* across temperature gradient shows that while WT has a K_d of 12.4°C, *coca1* has a K_d of only 8.8°C. K_d indicates the temperature at which the Ca^{2+} transient is half of its maximum. While the WT Ca^{2+} transient reaches it half maximum at 12.4°C, *coca1* needs the temperature to be approximately 4°C lower, indicating a compromised sensitivity towards low temperatures. Hill coefficient is a widely used parameter describing the effect of temperature decrease on the $[Ca^{2+}]_i$ in this case. Hill coefficients for the WT and

coca1 are 5.6 and 3.9 respectively. A smaller Hill coefficient indicates less responses, or in other words, more insensitive. Q_{10} describes the difference of $[Ca^{2+}]_i$ as a consequence of temperature change by 10°C. It was calculated to be 0.25 and 0.1 for WT and *coca1* respectively for the log phase of the curves. A smaller Q_{10} of *coca1* indicates less response compare to the WT when temperature changes by 10°C. All these three parameters show that *coca1* display a compromised sensitivity towards low temperatures. However, when temperature is below 6°C or above 18°C there is no significant difference in $[Ca^{2+}]_i$ between WT and *coca1*, indicating that *coca1* is only compromised in sensing ambient cool temperatures, especially in the range from 10°C to 14°C.

This observation is supported in YC3.6 system in *Arabidopsis* root, although the kinetics is different in root from those in leaves, they both show a compromised induction of $[Ca^{2+}]_i$ in response to low temperature. The difference in kinetics is within our expectation as it has been reported that cold triggers tissue and organ specific calcium signatures in *Arabidopsis*[92].

We further tested the performance of *coca1* toward other stimuli including ionic, osmotic and oxidative stimulus. *coca1* displays the same sensitivity as WT towards all the stimuli tested.

In summary, we conclude that through the forward genetic screen, we identified *coca1* as an *Arabidopsis* mutant with compromised sensitivity specific to ambient cool temperatures.

coca2 was identified through the same genetic screen. Different from *coca1, coca2* displays low specificity towards other stimuli tested. In addition to showing defects in response to cold, *coca2* also showed compromised $[Ca^{2+}]_i$ increase in response to sorbitol, $CaCl_2$ and NaCl. However, since cold, osmotic and salt stimuli all affect plasma membrane rigidity, this low specificity may indicate that *coca2* is defective in signaling downstream of membrane rigidity change. This is consistent with the observation that *coca2* also shows compromised $[Ca^{2+}]_i$ increase in response to temperatures below 6°C, which also triggers membrane rigidification. In addition, it has been well accepted that cold, drought and salt triggered responses share a broad range of similarities in plants, including the induction of overlapping responsive genes. Therefore, *coca2* is likely a mutant defective in sensing membrane rigidification triggered by low temperature.

2.4 Materials and methods

2.4.1 Growth conditions and media

Arabidopsis thaliana ecotype Col-0 constitutively overexpressing aequorin were used in this study. Plants were either grown in soil (Scotts Metro-Mix 200) or on half strength Murashige and Skoog salts (Caisson Labs, Logan, UT) supplemented with 1.5% sucrose (Sigma, St. Louise, MO) and 0.6% agar (Sigma) in controlled environmental rooms at 22°C under long day condition (16 hr white light/8 hr dark). The fluency rate of white light was ~100 $\mu mol.m^{-2}.s^{-1}$.

2.4.2 Genetic screen of coca

EMS mutagenized M2 *Arabidopsis* were screened for plants with reduced $[Ca^{2+}]_i$ increase after cold treatment. Seeds were surface sterilized with 2% plant preservative mix (PPM; Caisson Labs, Logan, UT) and stratified for 3 days at 4°C in the dark before being transferred to the growth room. Eight day old seedlings were used for aequorin bioluminescence imaging. Prior to imaging, seedlings were treated with 10uM coelenterazine (Gold Biotechnology, St. Louis, MO) and incubated in the dark for 8 hours to reconstitute aequorin. Aequorin bioluminescence imaging was performed using a ChemiPro HT system (Roper Scientific, Trenton, NJ) equipped with a light-tight box, a cryogenically cooled and back-illuminated CCD camera. The camera was controlled by WinView/32 (Roper Scientific, Trenton, NJ). 14°C deionized water was applied to seedlings and bioluminescence was recorded for 3 min. Images were analyzed using MetaMorph 6.3 (Molecular Devices, Sunnyvale, CA). Seedlings showing lower cold induced $[Ca^{2+}]_i$ increase were selected and M3 seeds were harvested. A total of 45,000 M2 plants were covered in this genetic screen.

2.4.3 Characterization of coca specificity

Responses of *coca* candidates towards other stimuli were examined to characterize the specificity. Eight day old seedlings were treated with various concentrations of sorbitol, NaCl, $CaCl_2$ and H_2O_2 solutions. Bioluminescence from each treatment was recorded for 5 min.

2.4.4 Yellow-Cameleon (YC3.6) based calcium imaging

coca mutants were crossed with wild type plants constitutively over-expressing yellow Cameleon 3.6 (YC3.6). YC3.6 based calcium imaging was conducted as described before[93]. 6 day old seedlings were used in this assay and 12°C water was used for cold treatment. Images were analyzed using MetaMorph Analyst (Molecular Devices, Sunnyvale, CA).

2.4.5 Physiological analysis of coca1 at low temperature

Seedlings were grown on modified MS medium (half strength MS basal salt micronutrient (Sigma, St. Louise, MO), half strength Gamborg's vitamin solution (Sigma, St. Louise, MO), 20mM NH_4NO_3, 18.8mM KNO_3, 1.2mM KH_2PO_4, 1.5mM $MgSO_4$, 1% agar (Invitrogen, Carlsbad, CA), 2.5mM MES hydrate (Invitrogen, Carlsbad, CA) supplemented with 0.1% sucrose. pH was adjusted to 5.7 with KOH.) 60mM $CaCl_2$ was supplemented as high Ca^{2+} treatment.

Seeds were surface sterilized with 15% bleach and sowed onto 50mm Petri dish (VWR, Radnor, PA) containing modified MS medium. After three-day stratification at 4°C in the dark, plates were transferred to 22°C constant light as control or to 14°C constant light as treatment and placed vertically. Plates were rotated 180° at noon every day. Images were taken after two weeks. Root length and fresh weight of the seedlings were measured.

Chapter 3 Physical mapping of COCA

3.1 Introduction

MutMap based cloning method was adopted to identify the causal mutation in *coca* mutants that leads to the defect in cold induced $[Ca^{2+}]_i$ increase phenotype[94]. In this method, *coca* mutants are directly crossed into their WT parental line. This gives rise to several advantages. First of all, by crossing mutants into the WT parents, who already carry homozygous aequorin, the segregation ratio of F2 seedlings displaying *coca* phenotype will be 1:4 rather than 1:16. Second, by using the parental line, MutMap minimizes the variation caused by a different ecotype background. According to Yuan *et. al*., *osmolarity induced* $[Ca^{2+}]_i$ *increase (osca1)* mutant phenotype could not be mapped if the mutant is crossed into ecotype Landsberg[87]. Therefore, MutMap is a method ideal for mapping mutants with subtle phenotypes.

Subsequent confirmation using derived cleaved amplified polymorphic sequences (dCAPS) was carried out and pinpointed that the causal mutation is within *Dynamin Related Protein 1A* (*DRP1A*). Complementation of functional DRP1A into *coca1* can rescue the defect in cold induced $[Ca^{2+}]_i$ increase in, further supports the causal relationship between DRP1A and *coca* phenotype. Subcellular localization and histochemical GUS studies showed that DRP1A is a plasma membrane localized protein express in cotyledons, true leaves and root of plants.

3.2 Results

3.2.1 MutMap based cloning of coca1

coca1 was crossed into parental line and F3 generation were used for physical mapping. We used pooled F3 population to represent their F2 parents because cold induced $[Ca^{2+}]_i$ increase is a transient and highly dynamic process, making it extremely difficult to score the phenotype in individual seedlings. Scoring phenotype from a pooled F3 population provides more consistent and reliable results.

Out of approximately 200 F3 lines, 40 F3 lines were found to display *coca1* phenotype and their genomic DNA were pooled and subject to 20X depth whole genome re-sequencing. Single nucleotide polymorphisms (SNPs) were identified by comparing the whole genome sequence of *coca1* to that of the WT parent. Indices of all SNPs were calculated and plotted against their chromosome coordinates (Figure 12). It is expected that for SNPs unlinked to the *coca1* phenotype, we would observe 50% of WT SNP and 50% of *coca1* SNP in the population. However, if the SNP is linked to the phenotype, the percentage will be biased to <50% of WT SNP and >50% of *coca1* SNP. If the SNP is causal to the *coca1* phenotype, we would expect 0% of WT SNP and 100% of *coca1* SNP.

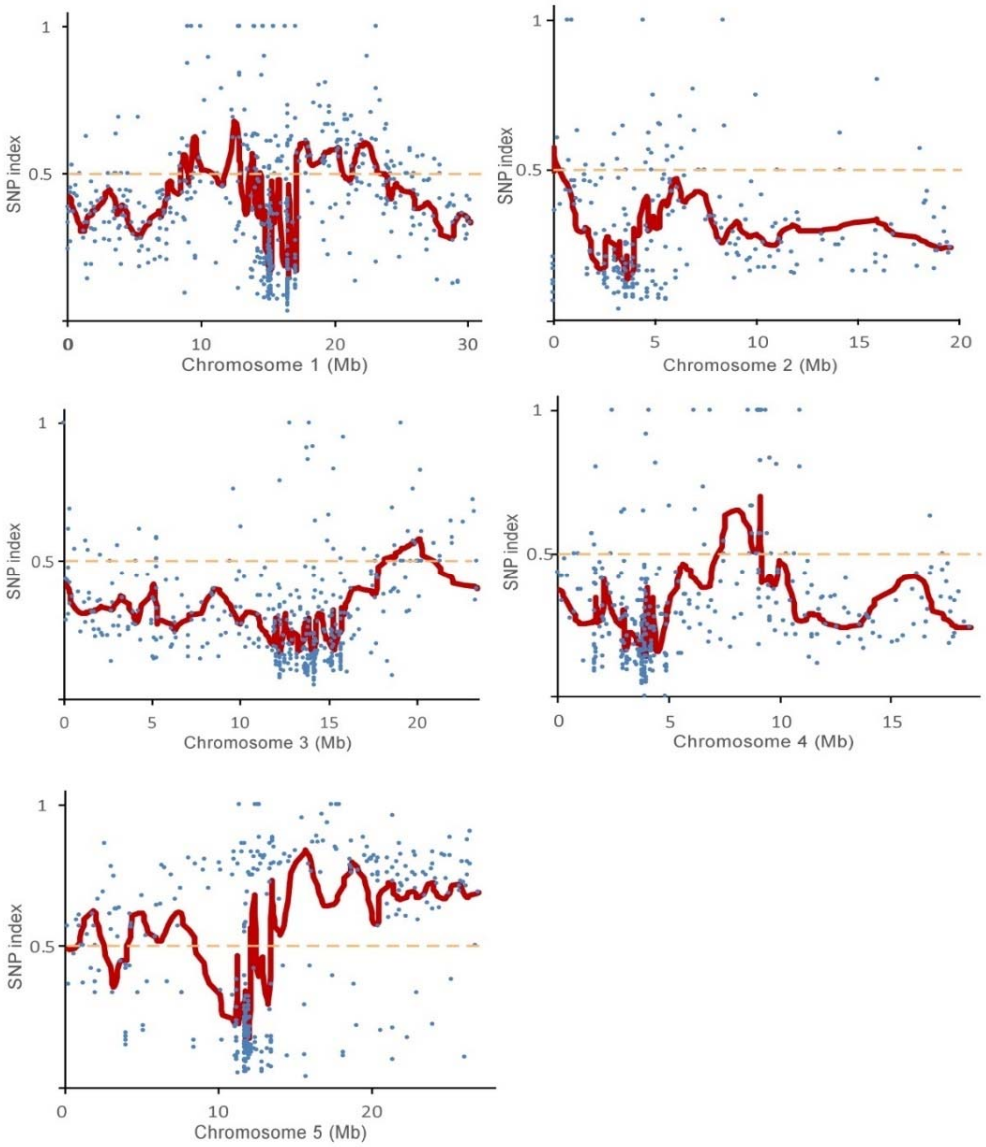

Figure 12 Identification of the genomic region harboring *coca1* causal mutation.

Plot of SNP indices of the five chromosomes in *coca1*. Blue dots represent SNPs in the genome against their SNP indices. Five consecutive SNP indices were averaged from a moving window and the window was shifted one SNP every time. The results were averaged the same way again for 5 times. Red lines represent the 5-time averaged results. Orange dashed lines indicate the 50% threshold.

As expected, one peak is found on the right arm of Chromosome 5. By analyzing the indices, we narrowed down the range of the causal SNP to be on the from 8069198 to 26404185.

3.2.2 Fine mapping of coca1 with dCAPS

To further pinpoint the causal mutation, fine mapping with dCAPS was performed (Figure 13).

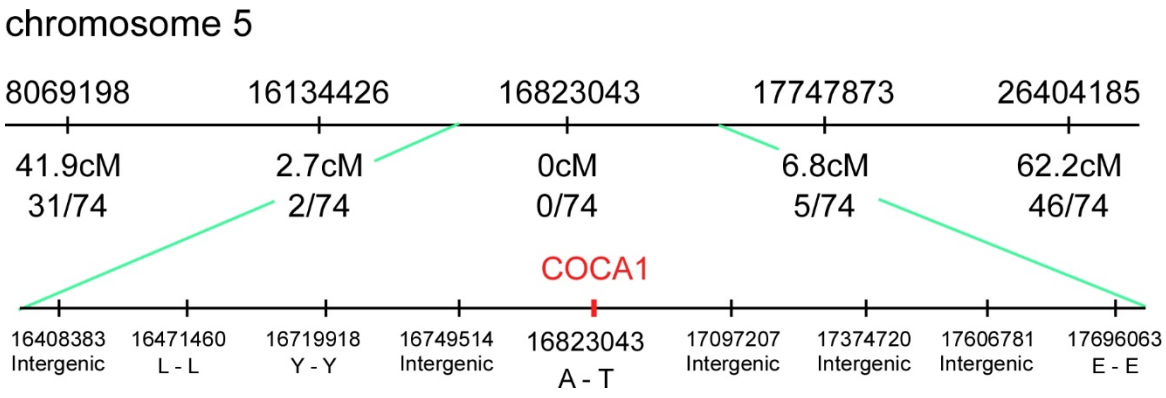

Figure 13 Fine mapping of *coca1*
Fine mapping using dCAPS defines the region of *coca1* in between 16134426 and 17747873 on chromosome 5. Detailed information of all SNPs within this range is listed in the magnified bar.

We found that *coca1* is located in between coordinate 16134426 and 17747873. Within this range, there are in total nine SNPs. Four out of these nine SNPs are within gene coding region. Only one SNP (16823043) causes a change in amino acid sequence of its protein product, dynamin related protein 1A (DRP1A) (AT5G42080). SNP 16823043 harbors a C→T transition, which is commonly found in EMS induced mutagenesis. This transition-type mutation leads to a change of

the amino acid codon from GCT to ACT, switching the amino acid from alanine (A) to threonine (T). While A carries a non-polar side chain, T carries a polar side chain. Therefore, SNP 16823042 may alter the function of its protein product.

3.2.3 Structural analysis of DRP1A

DRP1A encodes a protein of 611 amino acids. It consists of a GTPase domain, a middle domain and an effector domain (GED) according to Conserved Domains v. 3.1 (https://www.ncbi.nlm.nih.gov/Structure/cdd/wrpsb.cgi). The GTPase domain resides from the 42nd to the 248th amino acid. GTPase activity of DRP1A is triggered by protein homodimerization[95] and the homodimer interface resides from the 43rd to the 246th amino acid. Mutation of *coca1* is located at the 188th amino acid, which is within the GTPase domain and is predicted to be a conserved amino acid in the homodimer interface of the protein (Figure 14). Therefore, we predict that A188T may alter the ability of DRP1A to homodimerize which in turn affect the GTPase activity and the biological function of the protein.

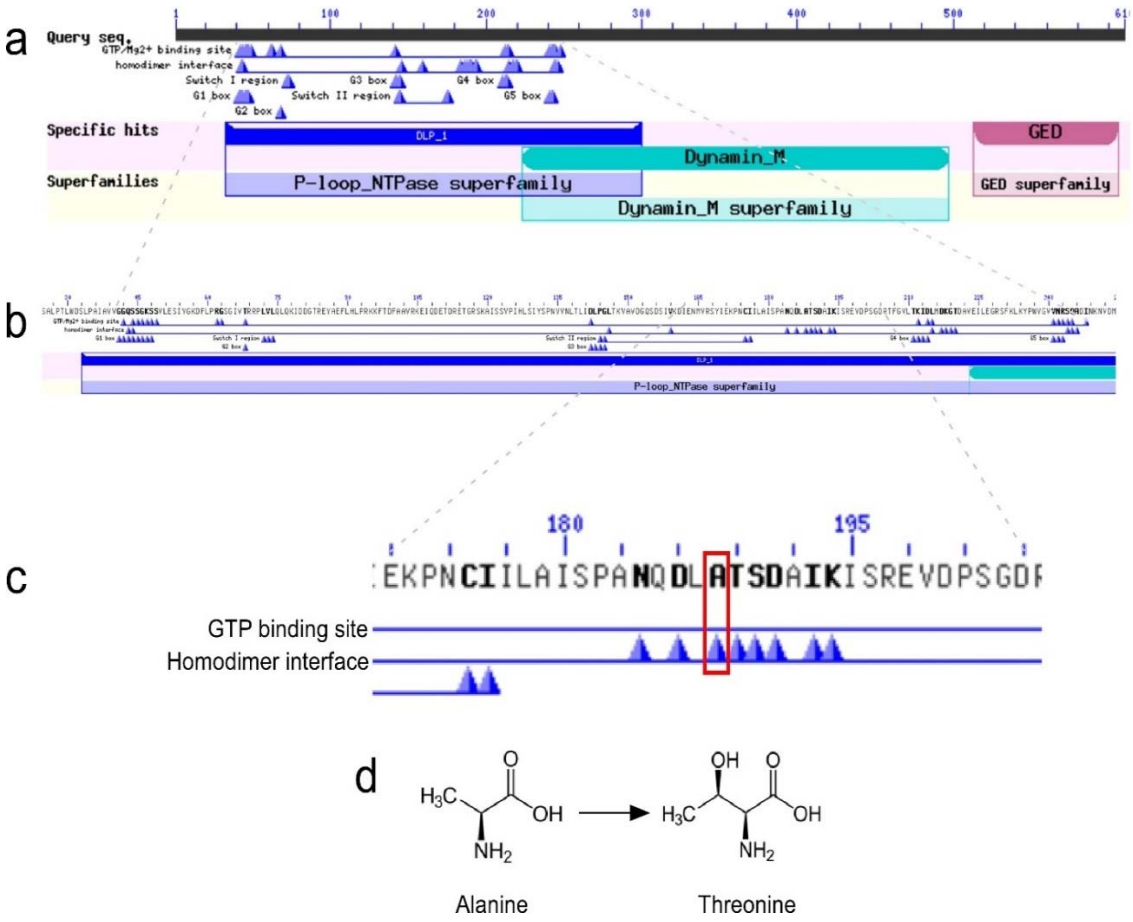

Figure 14 Sequence analysis of DRP1A.
a, Full illustration of domains in DRP1A. **b,** magnified view of GTPase domain and the homodimer interface domain. **c,** magnified view of the mutation site identified in *coca1*. The amino acid highlighted in the red box is the site of mutation. **d,** amino acid structures of the WT amino acid, alanine and the mutant amino acid, threonine.

3.2.4 Complementation of coca1 with DRP1A

To prove that *drp1a* is the causal mutation that leads to the *coca1* phenotype, complementation studies were performed. *pDRP1A::DRP1A* was transformed into *coca1* background. Cold induced $[Ca^{2+}]_i$ increase was examined in the transgenic lines. We found that *pDRP1A::DRP1A* can completely rescue the defect of $[Ca^{2+}]_i$ increase in *coca1* to the same level as in WT. On the other hand, *coca1-2*, which is a T-DNA knockout line of *coca1* displayed impaired cold induced $[Ca^{2+}]_i$ increase, resembling the phenotype of the *coca1* mutant (Figure 15).

Therefore, we conclude *drp1a* is responsible for the compromised cold induced $[Ca^{2+}]_i$ increase phenotype in *coca1*.

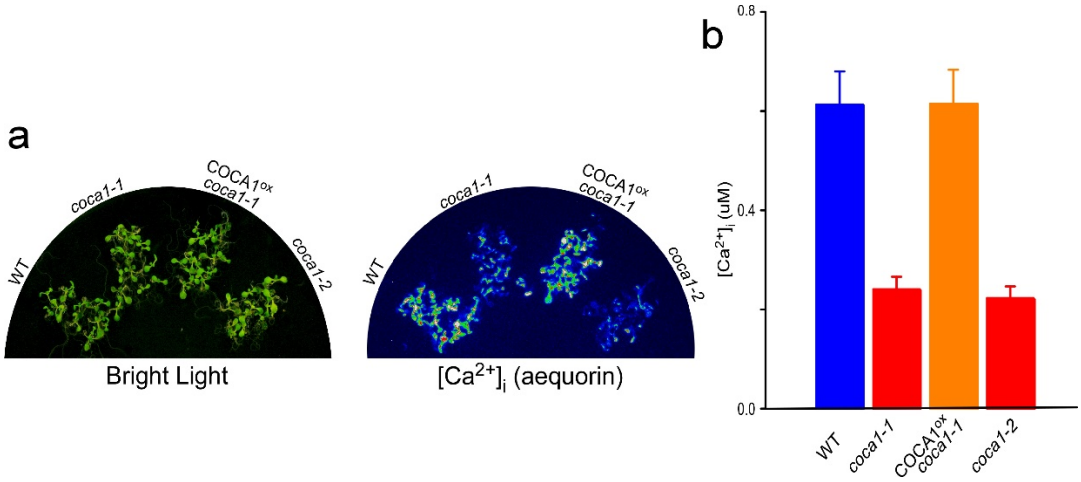

Figure 15 Complementation of *coca1*.
a, Light and bioluminescence images of *coca1* complementation with COCA1^{ox} *coca1-1*. *coca1-2* represents the T-DNA knock out line of *coca1.* **b,** Quantification of cold induced $[Ca^{2+}]_i$ increase in a. Three independently transformed complementation lines were examined and they all show the same phenotype. (error bar = s.e.m., n=30)

3.2.5 Expression pattern and subcellular localization

To study the tissue level expression of DRP1A, we transformed WT Col-0 with *pDRP1A::GUS*. We found that *DRP1A* is expressed in the cotyledon of eight-day old seedlings, as well as in the root (Figure 16). This is consistent with the genetic screen, which was imaged in the cotyledon of 8-day old seedlings. Further analysis at different developmental stages show that DRP1A is also expressed in the rosette leaves of adult plants, as well as the flowering tissues. Therefore, DRP1A is ubiquitously expressed throughout developmental stages.

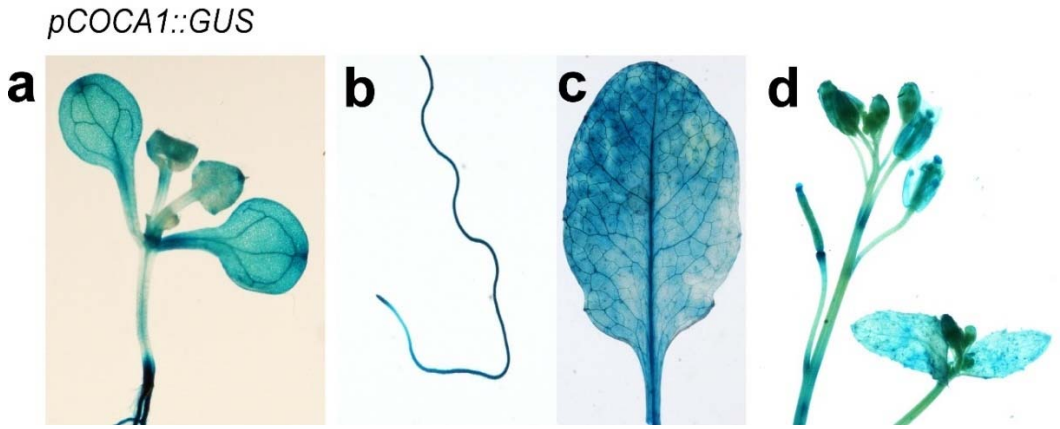

Figure 16 Histochemical studies of *DRP1A* expression pattern.
DRP1A is expressed in cotyledons **a,** and root **b,** of eight-day old seedlings, as well as rosette leaves **c,** and flowering tissues **d,** of adult plants.

Subcellular localization of DRP1A was studied by confocal analysis. DRP1A is mainly localized on the plasma membrane (Figure 17). Plamolysis shows that it is not located on the cell wall. In addition to plasma membrane localization, signals are also found in the cytosol as punctated dots, indicating the involvement in endocytosis. These are consistent with previous findings.

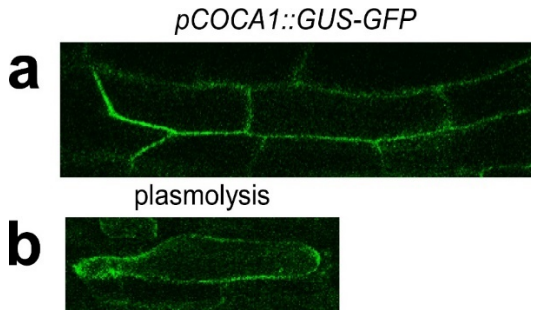

Figure 17 Subcellular localization of DRP1A.
Plasma membrane localization of DRP1A in seedlings expressing *pDRP1A::DRP1A-GFP*. GFP fluorescence was observed in the periphery of the turgid cells **a,** and plasmolysed cells **b,**. In addition, punctate dots were also observed in the cytosol consistent with the role of DRP1A in endocytosis.

3.3 Discussion

DRP1A is found to be responsible for the defect in cold induced $[Ca^{2+}]_i$ increase in *coca1*.

Mutation in *drp1a* leads to an amino acid change from alanine to threonine. The amino acid is located within the homodimer interface of the protein which also overlaps with the GTPase domain. It is known that the GTPase activity of DRPs are dependent on the nucleotide-dependent homo-dimerization through the homodimer interface[96]. Upon dimerization, the conformation of the GTPase domain of the partner DRP will be changed and thereby the GTPase activity will be activated[97]. This makes DRP unique compare to other regulatory G proteins which need GTP activating proteins (GAPs) to facilitate the GTP hydrolysis and guanine nucleotide exchange factors (GEFs) for the exchange of hydrolyzed GDP to GTP in order to enter a new hydrolysis cycle. In fact, the independence of

additional regulatory proteins (GAPs or GEFs) and the importance of G domain dimerization is highly conserved in the DRP family proteins[95,98]. Therefore, mutation of a highly conserved amino acid in the homodimer interface might reduce the efficiency of homodimerzation and subsequently the GTPase activity of the DRP1A.

Histochemical GUS staining shows that *DRP1A* is expressed in the cotyledons of eight-day old seedlings. This is consistent with the condition of our genetic screen, which carried out by imaging cotyledons of eight-day old seedlings. We also found that *DRP1A* is expressed in root of young seedlings, consistent with our YC3.6 imaging which was carried out by imaging roots of young seedlings. Therefore, the expression pattern of DRP1A is supportive to our cold induced $[Ca^{2+}]_i$ increase studies before. Furthermore, we observed expression of DRP1A in adult plants as well, including rosette leaves and flowering tissues. Indicating a role of DRP1A in adult plants too. Therefore, it is likely DRP1A confers ambient cool temperature sensitivity in *Arabidopsis* throughout developmental stages.

Subcellular localization studies revealed that DRP1A is localized to the plasma membrane as well as endosomes. The plasma membrane localization is consistent with the commonly accepted hypothesis that temperature sensing is mediated by components in the plasma membrane. The plasma membrane localization of DRP1A is also supported by various bioinformatics predictions, including Arabidopsis eGFP browser (http://bbc.botany.utoronto.ca/efp/cgi-bin/efpWeb.cgi?primaryGene), plant membrane database (AraMemmon:

http://aramemnon.uni-koeln.de/). Studies also show that DRP1A is enriched in lipid raft of the plasma membrane[99].

Therefore, DRP1A is identified to be the gene responsible for thermal sensing in *Arabidopsis*.

3.4 Materials and methods

3.4.1 Identification of DRP1A *using MutMap method*

Identification of *coca1* was carried out using MutMap method as described[94] with modifications. Briefly, *coca1* mutant was crossed with wild type parental plants (Col_{AQ}). The resulting first filial generation (F1) plants were self-pollinated. Two hundred F2 progeny were grown and F3 seeds were collected. Cold induced $[Ca^{2+}]_i$ increase was examined using pooled F3 progeny. At least 15 F3 seedlings derived from each F2 plants were imaged as a pool for Cold induced $[Ca^{2+}]_i$ increase. Lines with all F3 seedlings exhibiting lower Cold induced $[Ca^{2+}]_i$ increase were considered as homozygous *coca* in F2 generation and their DNA was extracted. DNA from all homozygous *coca* seedlings were pooled in equal amount to reach a final quantity of 10 µg for whole genome re-sequencing.

3.4.2 Fine mapping using dCAPS

Derived cleaved amplified polymorphic sequences (dCAPS) markers were designed using dCAPS finder 2.0 (http://helix.wustl.edu/dcaps/dcaps.html) for fine mapping.

Table 1 Primers for dCAPS analysis

SNP coordinate	Primer sequence 5'-3'	Restriction Enzyme
Chr5-8069198 F	ATCCATGGCTGAGGAAAGAGTCGA	SalI
Chr5-8069198 R	AGTTGAATTTTCCCTTGTGCAC	
Chr5-16134426 F	CTTCTTCTTCTTCATCTTCGCC	PstI
Chr5-16134426 R	AGTTTCTTCCTTGCTCAAACTGCA	
Chr5-16823043 F	TGCTCACCCGATGGATCAACCTC	AluI
Chr5-16823043 R	CATTTTGGCAATCTCACCTGCAAACCA AGATCTA	
Chr5-17747873 F	GGAAGCTGCAAGAGCTCAAGCT	HindIII
Chr5-17747873 R	TCAAGGAATTCCGATATTGGGG	
Chr5-26404185 F	CTGTTCTTCATGCGGGTTCTCG	XhoI
Chr5-26404185 R	AGAGAGCGAATCTGTTGGCTCG	

3.4.3 Molecular cloning

Gateway cloning system was used in this study. cDNA of DRP1A (*cDRP1A*), genomic DNA of DRP1A (*gDRP1A*) and 2.5 kb of the promoter region (*pDRP1A*) were amplified from cDNA and genomic DNA respectively. Amplified fragments were first cloned into entry vectors and then further recombined into corresponding destination vectors using LR recombinase (Invitrogen).

Table 2 Primers used for molecular cloning

Primer name	Primer sequence 5'-3'
pDRP1A F	CGTCCTCTACTCCTCGTTTCCCC
pDRP1A R	GGAGATGGAGATCAAGAGAAGG
cDRP1A F	ATGGAAAATCTGATCTCTCTGG
cDRP1A R (stop codon)	TCACTTGGACCAAGCAACAGCATCGATC
cDRP1A R (no stop codon)	CTTGGACCAAGCAACAGCATCGATC
pDRP1A F (+attP)	GGGGACAAGTTTGTACAAAAAAGCAGGCTG GGGAGATGGAGATCAAGAGAAGG
gDRP1A R (stop codon; +attP)	GGGGACCACTTTGTACAAGAAAGCTGGGTT TCACTTGGACCAAGCAACAGCATC
gDRP1A R (no stop codon; +attP site)	GGGGACCACTTTGTACAAGAAAGCTGGGTC TTGGACCAAGCAACAGCATCG

Transgenic plants were generated through *Agrobacterium* mediated transformation. Plants in T3 generation were genotyped using the selectable marker on the constructs and homozygous lines were used in this study.

Table 3 Constructs and transgenic Arabidopsis

construct	**Entry Vector**	**Destination Vector**	***Arabidopsis* Background**
p35S::COCA1	pCR8/gw/topo	pGWB 502	*coca1*
pCOCA1::COCA1	pDONR 207	pMDC 99	*coca1*
pCOCA1::COCA1-GFP	pDONR 207	pMDC 107	Col-0
pCOCA1::GUS	pCR8/gw/topo	pGWB 533	Col-0

3.4.4 Histochemical GUS activity

The histochemical staining for β-glucuronidase (GUS) activity was done with *pCOCA1::GUS* expressing *Arabidopsis.* Expression pattern in seedlings as well as adult plants were examined. Brief vacuum infiltration was applied prior to staining for adult plants. Staining solution (0.1M $NaPO_4$ pH7, 10mM EDTA, 0.1% Triton X-100, 3mM $K_3Fe(CN)_6$, 0.2mM X-Gluc) was removed after incubating at 37°C in the dark, 6 hrs for seedlings and overnight for adult plants. De-staining was done using 50% ethanol. Three independent lines were examined in this study.

3.4.5 Subcelluar localization study

Subcellular localization of DRP1A was studied using *Arabidopsis* expressing *pCOCA1::COCA1-GFP*. Plants expressing *p35S::GFP* was used as control. Seven day old seedlings were taken for confocal imaging with Zeiss 510 Inverted confocal microscope. Plasmolysis was done by treating seedlings with 0.8M sorbitol solution.

Chapter 4 Molecular mechanisms of *coca1* mediated low temperature perception in plants

4.1 Introduction

As described before, a commonly accepted model of low temperature sensing in plants involved a rapid membrane rigidification, followed by a drastic increase of transient $[Ca^{2+}]_i$ increase through plasma membrane localized calcium channels. This transient $[Ca^{2+}]_i$ increase in turn triggers the re-organization of cytoskeleton which may potentiate the sensitivity of cold activated channels towards low temperature. With the identification of DRP1A as potential ambient cool temperature mediator, we would like to understand the relationship between DRP1A and the current model of low temperature sensing in plants.

The relationship between DRP1A and membrane rigidity, cytoskeleton re-organization were examined.

4.2 Results

4.2.1 DMSO triggered $[Ca^{2+}]_i$ increase

Because DMSO is known to trigger membrane rigidification and expression of COR genes, we first tested if DMSO also triggers $[Ca^{2+}]_i$ increase[34]. Eight-day old seedlings were treated with 0.5%, 1%, 2% and 3% DMSO. We found that there was no significant influence of DMSO on the seedlings when the concentration is below 2% (data not shown). However, when the seedlings are treated with 3% DMSO, there is a significant increase of $[Ca^{2+}]_i$ (Figure 18). Interestingly, this

DMSO triggered $[Ca^{2+}]_i$ increase is not impaired in *coca1*. In order to exclude the possibility that this DMSO triggered $[Ca^{2+}]_i$ increase is not due to the membrane leakage caused by 3% DMSO, we pretreated the seedlings with calcium channel blocker, lanthanum chloride ($LaCl_3$). Pre-treatment of seedlings with 1mM $LaCl_3$ for 2 hours completely abolished DMSO triggered $[Ca^{2+}]_i$ increase in both WT and *coca1*, indicating that DMSO triggered $[Ca^{2+}]_i$ increase is mediated by plasma membrane located calcium channels.

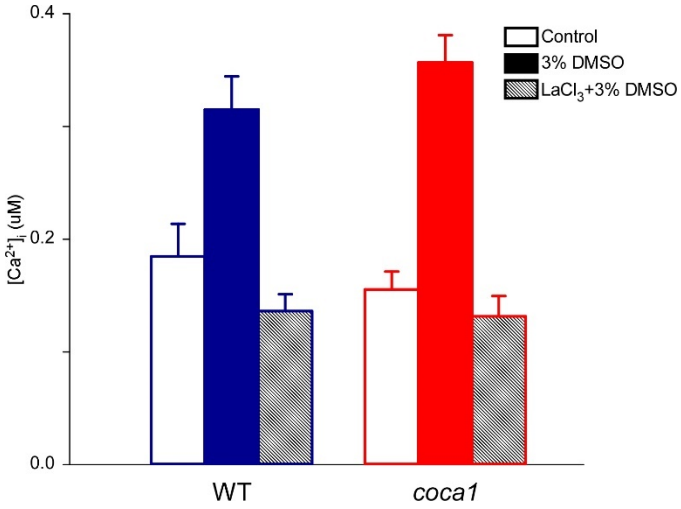

Figure 18 Effects of DMSO on $[Ca^{2+}]_i$ increase.
Open columns represent water control. Filled columns represent 3% DMSO treatment. Shaded columns represent 1mM LaCl3 incubation for 2 hrs followed by 3% DMSO treatment. (mean ± s.e.m. n=30)

4.2.2 DMSO potentiates cold induced $[Ca^{2+}]_i$ increase in Arabidopsis

To test if DMSO mediated membrane rigidification modifies cold induced $[Ca^{2+}]_i$ increase, we pre-treated seedlings with 1% DMSO for 2 hours before applying low temperature treatment.

After DMSO pre-treatment, we observed stronger responses toward low temperature treatment in both WT and *coca1*. Interestingly, while WT showed approximately 1.28 fold increase of $[Ca^{2+}]_i$ increase compare to the water control, *coca1* displayed approximately 2 folds of $[Ca^{2+}]_i$ increase (). Indicating DMSO triggered membrane rigidification can partially alleviate the defect in *coca1* but not completely.

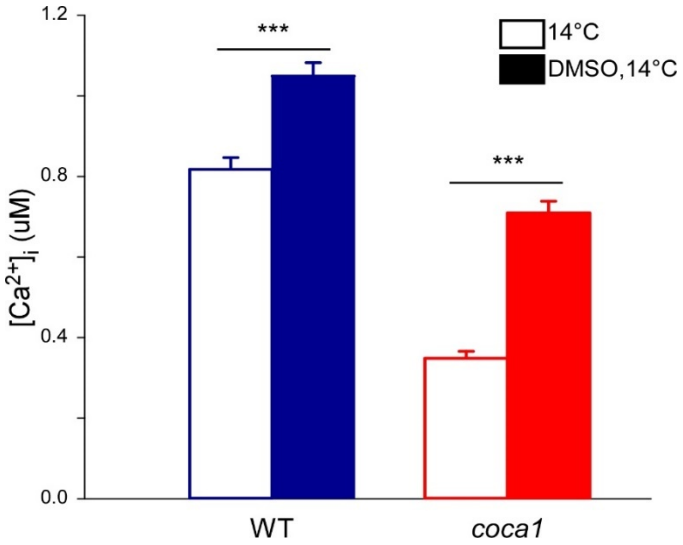

Figure 19 Effects of DMSO on cold induced $[Ca^{2+}]_i$.
Open column, seedlings pre-treated with water as control. Filled column, seedlings pre-treated with 1% DMSO for 2hr. Afterwards, 13.5°C water was applied to the seedlings and $[Ca^{2+}]_i$ increase was recorded. (mean ± s.e.m., n=30)

4.2.3 Microtubule reorganization potentiates cold induced $[Ca^{2+}]_i$ increase

To test the effect of microtubule re-organization on cold induced $[Ca^{2+}]_i$ increase, we treated seedlings with 400μM colchicine and recorded $[Ca^{2+}]_i$ increase as a consequence. However, even after cumulative recording for 30 min, we did not observe any significant $[Ca^{2+}]_i$ increase triggered by 400μM colchicine (data not shown). Therefore, 400μM colchicine itself does not trigger $[Ca^{2+}]_i$ increase in our experimental conditions. However, after pre-treatment of 400μM colchicine for 2hrs, cold triggered a more intensified $[Ca^{2+}]_i$ increase. The folds of increase in WT and in *coca1* are both approximately 1.3 fold (Figure 20).

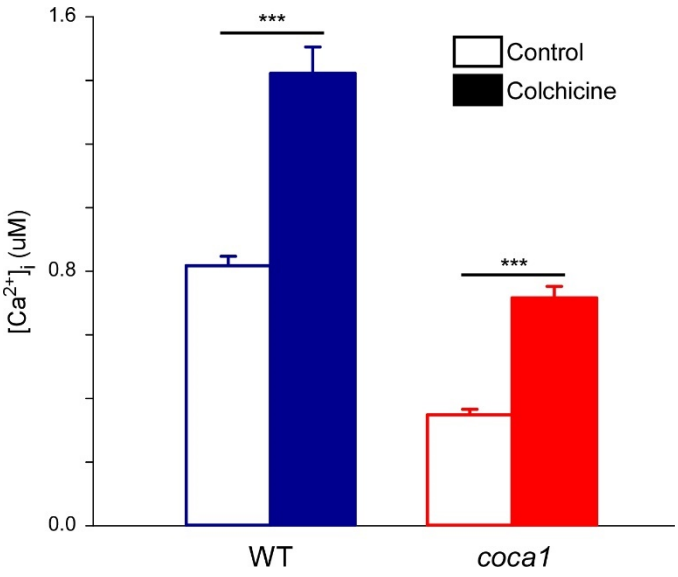

Figure 20 Effect of colchicine on cold induced $[Ca^{2+}]_i$ increase.
Open column, seedlings incubated with 0.1% DMSO for 2 hrs as control before 13.5°C cold treatment. Filled column, seedlings incubated with 400μM colchicine for 2 hrs, before 13.5°C cold treatment. (error bar = s.e.m., n=30)

4.2.4 Dynasore attenuates cold induced $[Ca^{2+}]_i$ increase

To test if the GTPase activity of DRP1A is required in the low temperature sensing, we treated seedlings with Dynasore. Dynasore is commonly used in animal researches as a membrane permeable inhibitor of dynamin. It blocks the GTPase activity of dynamin and thereby renders it un-functional.

Seedlings were pre-treated with 100 μM Dynasore for 2 hours and in the control group, seedlings were treated with 1% DMSO for 2 hours. This is due to the low solubility of Dynasore in DMSO. As expected, we found that Dynasore can inhibit cold induced $[Ca^{2+}]_i$ increase compare to 1% DMSO treated samples (Figure 21).

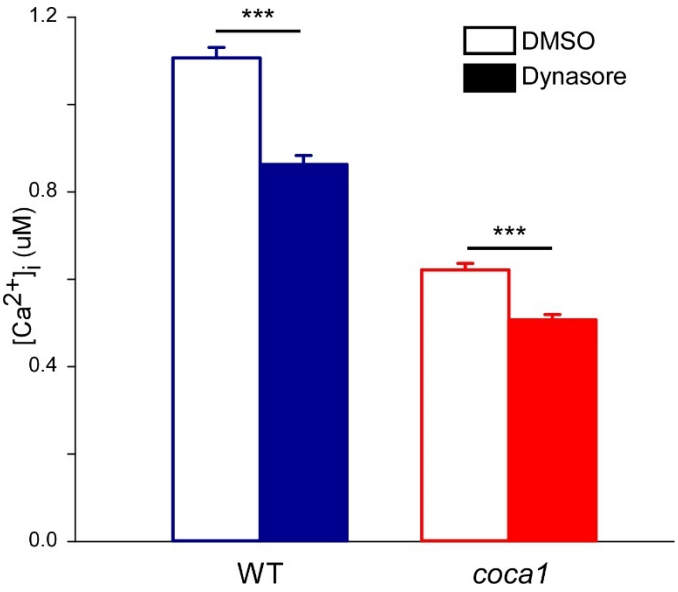

Figure 21 Effect of Dynasore on cold induced $[Ca^{2+}]_i$ increase. Open column, seedlings were incubated in 1% DMSO for 2 hrs as control. Filled column, seedlings were incubated in 100 μM Dynasore for 2 hrs. 13.5C water was applied to seedlings after the incubation. (mean ± s.e.m., n=30)

4.3 Discussion

4.3.1 DRP1A function in relation to membrane rigidification and cytoskeleton re-organization

In order to understand molecular mechanisms of how DRP1A mediates low temperature sensing and its relationship with the known components in thermal sensory steps in plants, we carried out pharmacological studies targeting known components involved in early steps of low temperature sensing.

First of all, we investigated the effects of DMSO on cold induced $[Ca^{2+}]_i$ increase. DMSO is a well-known plasma membrane rigidifier and treatment of DMSO can trigger low temperatures responses including the induction of *COR* genes[34]. We found that below 2% concentration, DMSO does not trigger observable $[Ca^{2+}]_i$ increase either in the WT or *coca1*. Based on previous studies, Whalley et. al., demonstrated that 2% DMSO triggers approximately 0.6μM increase of $[Ca^{2+}]_i$ from resting calcium level[100]. This discrepancy could be due to the different methods used for intracellular Ca^{2+} measurement. In Whalley's study, treatments were applied onto individual seedlings placed in a cuvette, and the bioluminescence of individual seedlings was recorded accordingly using spectrometer[100]. However, in our system, Ca^{2+} signals are measured with seedlings grown in petri dishes and are placed about 0.5 meter away from a camera. Therefore, the discrepancy between their results and ours may be due to a higher resolution of their system.

However, we do observe a significant $[Ca^{2+}]_i$ increase at 3% DMSO both in the WT and *coca1*. Interestingly, the elevation of $[Ca^{2+}]_i$ in *coca1* is approximately the same as that in the WT, indicating that mutation of *DRP1A* in *coca1* does not affect membrane rigidification triggered $[Ca^{2+}]_i$ increase. Therefore, it is possible that membrane rigidification is downstream of DRP1A in low temperature perception, or alternatively, DMSO at 3% concentration causes damage on the plasma membrane which leads to the leakage of calcium ions. To test if DMSO triggered $[Ca^{2+}]_i$ increase is through calcium channels or is a result of membrane leakage, we treated the seedlings with $LaCl_3$, which is a calcium channel blocker. We found that pre-treatment with $LaCl_3$ can completely block DMSO triggered $[Ca^{2+}]_i$ increase. This excludes the possibility that DMSO causes plasma membrane damage at 3% concentration. An alternative explanation is that DMSO triggered $[Ca^{2+}]_i$ increase is independent of DRP1A mediated temperature sensing. To test this possibility, we pre-treated seedlings with DMSO and subsequently examined their responses toward cold.

One percent DMSO was used for the treatment. It has been that 1% DMSO induces the expression cold responsive gene, but cause no damage to seedlings. Furthermore, it does not trigger significant $[Ca^{2+}]_i$ increase on its own. After 2 hr incubation with 1% DMSO, we observed stronger $[Ca^{2+}]_i$ increase upon cold treatment in both WT and *coca1*, indicating a potented low temperature sensitivity a result of chemical induced membrane rigidification. Interestingly, the potentiation

in *coca1* is stronger than that in the WT, indicating that membrane rigidification can partially rescue the defect in *coca1*.

Therefore, we suggest here that DRP1A functions upstream of membrane fluidity change. DRP1A may mediate membrane rigidification at low temperature, leading to a change in membrane curvature as is a classic function of dynamins in clathrin-mediated endocytosis. This change in membrane curvature may ultimately lead to the activation of calcium channels embedded in the plasma membrane. The reason why 1% DMSO can only partially rescue cold induced $[Ca^{2+}]_i$ increase in *coca1* is probably because 1% DMSO is not sufficient for fully rigidify the membrane. However, although high concentration of DMSO might lead to stronger rigidification, it will also trigger $[Ca^{2+}]_i$ increase even without low temperature treatment, leading an altered Ca^{2+} homeostasis.

Secondly, we studied the effect of microtubule re-organization on cold induced $[Ca^{2+}]_i$ increase. We found that pre-incubation of seedlings with 400μM colchicine does not trigger $[Ca^{2+}]_i$ increase. However, pretreatment of seedlings with 400μM colchicine potentiates the subsequent cold induced $[Ca^{2+}]_i$ increase.

It has been well accepted that microtubule re-organization is involved in many signaling events[48]. Mazars *et. al.* showed that pre-treatment of tobacco protoplasts with microtubule disrupting chemicals including colchicine, vinblastin and oryzalin can all potentiate the subsequent cold induced $[Ca^{2+}]_i$ increase[49]. Orvar and Sangwan *et. al.* demonstrated that treatment with microtubule disrupting chemicals can trigger cold response at room temperature[34]. However, in both our

and Mazars' studies, no significant $[Ca^{2+}]_i$ increase was observed without cold treatment. One possibility is that without cold treatment, the $[Ca^{2+}]_i$ increase caused by microtubule disruption is too weak to be detected by our system.

There are two possible mechanisms behind the potentiation of cold induced $[Ca^{2+}]_i$ increase after colchicine treatment. Either microtubule disruption is upstream of cold induced $[Ca^{2+}]_i$ increase and therefore is necessary before the signal can be relayed onto calcium channels; or microtubule disruption is triggered by cold induced $[Ca^{2+}]_i$ increase which further potentiates the activity of cold activated calcium channels. According to previous studies, microtubule disruption is much slower compare to the $[Ca^{2+}]_i$ increase, therefore, it is unlikely to be located upstream of the signaling pathway.

4.3.2 Dynamin as a mediator of thermal perception in plants

Dynamin is originally identified as a co-purified 100kD protein with microtubules from calf brain[101]. It is suggested to function as a microtubule activated mechanochemical GTPase which generates force on microtubules during vesicle transport[102]. Later, a temperature dependent paralytic mutant in *Drosophila melanogaster* (*shibire*) was identified through a forward genetic screen[103] and the mutation was subsequently mapped to a dynamin encoding gene[104]. In *shibire*, endocytic vesicles cannot be pinched off from the plasma membrane under non-permissive temperatures, and therefore, vesicles carrying neurotransmitters are depleted at the synaptic terminals, leading to the paralytic phenotype. However, upon returning to permissive temperatures, endocytosis

resumes[105]. Since then the classical model of dynamin in endocytosis has been established. In support of this hypothesis, *in vitro* studies were carried out and it is found that dynamin can self-assemble to a ring-like structure around artificial lipids. The self-assembly of dynamin is independent of GTP hydrolysis, which is required for the constriction and pinching off of the vesicle from the plasma membrane[106]. Since then, more diversified function of dynamins and dynamin like proteins (DRPs) have been described. These functions can be summarized into a general function of sensing and generation of membrane curvatures[95]. In support of this hypothesis, dynamins are found to be associated with cytoskeleton meshwork in structures like podosome and lamellipodia. In these situations, the interaction between dynamin and cytoskeleton is suggested to help the modeling and generation of membrane curvatures.

A classical dynamin consists of 5 motifs: 1. A GTPase domain binds GTP and hydrolyze it from GTP to GDP. 2. A middle domain that serves at dimerization interface. 3. A Pleckstrin homology (PH) domain that mediates the interaction between dynamin and the acidic phospholipids in the cytosolic side of the plasma membrane. 4. A GTPase effector domain (GED) that interacts with the GTPase domain. Mutation in the GED leads to the suppression of GTPase domain activity. 5. A proline rich domain (PRD) which localizes dynamin to the functional sites and coordinated the interaction with other proteins.

In plants, there are 16 dynamins like proteins in Arabidopsis[107]. They are grouped into 5 classes based on their phylogeny and presence of functional

domains. They are involved in diversified functions including cell plate formation, mitochondrion division, chloroplast division, and cytokinesis. Recently Arabidopsis DRPs are found to involved in various stress responses. DRP2B was shown to be involved in plant immune responses[108]. In addition, DRP1E was found to protect *Arabidopsis* from freezing stress[109]. In this study, *drp1e* knock out plants were not able to develop freezing tolerance after prolonged acclimation and therefore are more susceptible. In line with this observation, DRP1E is found to be enriched in detergent resistant plasma membrane micro-domains after cold acclimation[99]. Microdomains are highly packed and organized regions consist of sterols, glycosphingolipids and proteins involved in signaling and vesicular trafficking. Therefore, DRP1E functions in the lipid rafts to signal the development of freezing

As the mutation site of *coca1* is located on a conserved amino acid of the homodimer interface of DRP1A, while the GTPase activity is dependent on the dimerization, this mutation in *coca1* likely affects the GTPase activity and thereby cause the *coca1* phenotype. To test if the GTPase activity of DRP1A is required for triggering cold induced $[Ca^{2+}]_i$ increase, we treated seedlings with Dyansore for 2 hours before cold treatment. As expected, treatment of seedlings with dynasore attenuates cold induced $[Ca^{2+}]_i$ increase. Therefore, the GTPase activity is required for the cold perception mediated by DRP1A.

In summary, we propose that DRP1A mediates thermal perception by triggering membrane rigidification, which in turn generates membrane curvature, activate Ca^{2+} channels and lead to cold induced $[Ca^{2+}]_i$ increase.

However, an alternative explanation is that DRP1A triggered cold activated endocytosis and through endocytosis signaling, mediates low temperature perception.

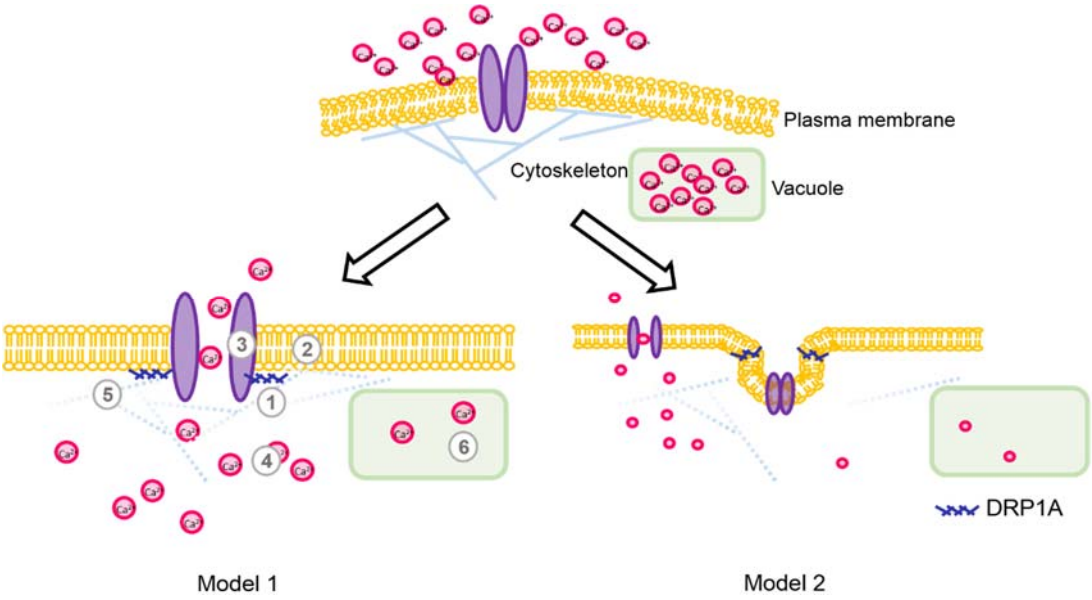

Figure 22 Working models of DRP1A mediated thermal perception in plants
In model 1, DRP1A perceives low temperature (1) and lead to membrane rigidification (2). Rigidification will change the curvature of the plasma membrane which generates a mechanical force and opens up the Ca^{2+} channel (3). Activation of Ca^{2+} channels allows Ca^{2+} to move down concentration gradient (4). This increase in $[Ca^{2+}]_i$ will further disrupt cytoskeleton stability (5) and signals the efflux of Ca^{2+} from vacuoles (6). In model 2, DRP1A triggers endocytosis in response to cold and lead to the activation of cold induced $[Ca^{2+}]_i$ increase through endocytosis signaling.

4.4 Materials and methods

Seedlings were grown in 15 X 100 mm petri dishes (VWR, Radnor, PA) for 8 days on half strength MS medium under long day condition. To avoid the influence of circadian, all experimental treatments were done at the same time of a day. Aequorin reconstitution was done 9 o'clock in the morning. Each petri dish

was evenly sprayed with 3ml of 10μM Coelenterazine and incubated in the dark. All chemical treatments were applied at 3 o'clock in the afternoon and incubated for an additional 2 hrs in the dark. All working solutions were prepared by diluting stock solutions into half MS medium. Cold treatment was done by applying 50 ml of 13.5°C deionized water gently into the petri dish. Aequorin bioluminescence was recorded for 3 min. After 1 hr recovery, total aequorin was measured by applying 1M $CaCl_2$ supplemented with 10% EtOH.

4.4.1 DMSO induced $[Ca^{2+}]_i$ increase

DMSO (Invitrogen, Carlsbad, CA) of desired concentration was prepared and 50 ml of the DMSO solution was applied gently. Fifty ml of room temperature water was applied gently into the petri dish as control. During the $LaCl_3$ inhibition study, 3ml of 1mM $LaCl_3$ was sprayed evenly onto each petri dish, and 3ml of water was sprayed at the same time as control. After 2 hr incubation, 50ml of 3% DMSO was applied as treatment.

4.4.2 DMSO effects on cold induced $[Ca^{2+}]_i$ increase

DMSO treatment were performed at 3 p.m. by spraying 3ml of 1% DMSO evenly onto each petri dish. Control group was sprayed with 3ml of water. After 2 hr incubation in the dark at room temperature, cold treatment was applied by gently pouring 50 ml of 13.5°C water.

4.4.3 Colchicine treatment

DMSO was used as a solvent to prepare colchicine (Invitrogen, Carlsbad, CA) stock solution (400mM). Colchicine treatment was done by spraying 3ml of 1000-fold diluted stock solution onto each petri dish. Control group was treated with 0.1% DMSO.

4.4.4 Dynasore treatment

DMSO was used as a solvent to prepare Dynasore (Invitrogen, Carlsbad, CA) stock solution (100mM). Dynasore treatment was done by spraying 3ml of 100-fold diluted stock solution onto each petri dish. Control group was treated with 1% DMSO.

Chapter 5 Physical mapping of coca2

MutMap based cloning was performed with *coca2* mutant. A peak is identified on Chromosome 1 from coordinate 25305029 to 28465805 (**Error! Reference source not found.**). Further analysis with dCAPS is needed to characterize the gene responsible for the defects.

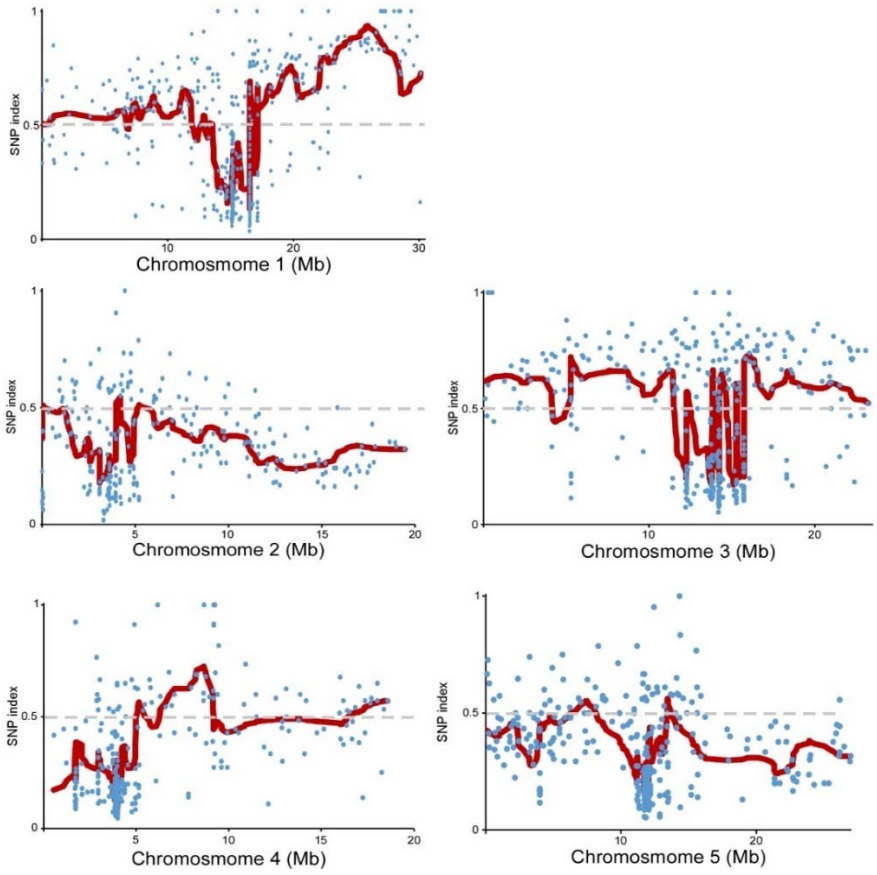

Figure 23 Identification of the genomic region harboring *coca2* causal mutation using MutMap.
Plot of SNP indices of the five chromosomes in *coca2*. Blue dots represent SNPs in the genome against their SNP indices. Five consecutive SNP indices were averaged from a moving window and the window was shifted one SNP every time. The results were averaged the same way again for 5 times. Red lines represent the 5-time averaged results. Grey dashed lines indicate the 50% threshold.

Chapter 6 Discussion and future perspectives

6.1 Discussion

Global warming has significantly altered the patterns of temperatures across the world. Unlike animals, who are able to move away from unfavorable temperatures, plants as sessile organisms are more vulnerable. As expected, disturbance of growth, development, and geographic distribution of plants have been reported along with loss of agricultural crop production. Intensive studies have been carried out to understand plant temperature responses, leading to the characterization of signaling pathways including acclimation and vernalization. However, due to various difficulties, the molecular mechanisms of plant thermal perception remain unknown. In this study, we adopted a novel Ca^{2+}-imaging based forward genetic screen and successfully identified mutants with defects in cold induced $[Ca^{2+}]_i$ increases. We found that *coca1* is defective only towards ambient cool temperature sensing and displays compromised fitness at 13°C as a consequence. Through map based cloning, *COCA1* is found to encode DRP1A protein. Our studies suggest that DRP1A may function in modification of membrane curvature in response to temperature changes and thus mediate the activation of Ca^{2+} channels. In conclusion, DRP1A is a component mediating low temperature induced $[Ca^{2+}]_i$ increases and thereby enables plants to better adapt to low temperatures. We report in this study the identification and characterization

of a component in mediating cold induced $[Ca^{2+}]_i$ increase for the first time and open up a new function of DRP1A.

6.1.1 The coca1 mutant is specifically compromised in ambient cool temperature sensing based on Ca^{2+} imaging

It has been known for over 20 years that cold triggers a transient increase of $[Ca^{2+}]_i$ in plants[40,41]. Due to the highly conserved function of $[Ca^{2+}]_i$ increase in mediating thermal perception in animals, it has been long speculated that these $[Ca^{2+}]_i$ increases may also mediate thermal perception in plants[79-81,83,84,110]. Indeed, blocking cold induced $[Ca^{2+}]_i$ increase attenuates COR gene expression[40]. However, the molecular components of cold induced $[Ca^{2+}]_i$ increase remain unknown, rendering it impossible to further study the role of $[Ca^{2+}]_i$ increases in thermal perception.

The lack of information of the molecular identity of the thermal sensory apparatus prompt us to design forward genetic screen. In contrast to traditional genetic screen, in which the phenotype scored takes hours to develop, we adopted a Ca^{2+}-imaging based genetic screen. Cold induced $[Ca^{2+}]_i$ increase occurs within less than a second after cold treatment, which provides the advantage of a narrow screening spectrum and thus greatly increases the resolution of signaling events upstream of $[Ca^{2+}]_i$ increases. On the other hand, due the dynamic nature of cold induced $[Ca^{2+}]_i$ increases, the variation of Ca^{2+} signals as well as the potential signal from other stimuli during the treatment introduced considerable noises to this genetic screen, which caused a large number of false positive candidates. This

is probably why for over 20 years, regardless of intensive trials, the molecular mechanisms of plant thermal perception remain unknown.

Through Ca^{2+}-imaging based genetic screen, we successfully identified mutants with compromised cold induced $[Ca^{2+}]_i$ increases (*coca*). Among the *coca* mutants identified, we describe *coca1* as a mutant specific for mediating ambient cool temperature induced $[Ca^{2+}]_i$ increase. *coca1* is fully responsive to other stimuli including osmotic, ionic and oxidative in terms of $[Ca^{2+}]_i$ increases, and therefore is defective in only perceiving temperature changes. In addition, *coca1* shows normal response to temperatures below 6°C, indicating the presence of multiple signaling pathways in plant thermal sensing which are activated at different temperature thresholds, as is the case in animal thermal sensing and *coca1* mediates specifically ambient cool temperature perception. Through physiological analysis, *coca1* seedlings grown at ambient cool temperature for 3 weeks display shorter roots compare to the WT. Thus, *coca1* also confer lower fitness at physiological level.

Therefore, through the novel Ca^{2+}-imaging based genetic screen, we successfully identified mutants with defects specifically in ambient cool temperature induced $[Ca^{2+}]_i$ increase for the first time.

6.1.2 Mutation in DRP1A is responsible for compromised cold induced $[Ca^{2+}]_i$ increase in coca1

Through personal communication with Prof. Knight (unpublished data), we noticed that by genetic cross of *coca1* into certain ecotypes of *Arabidopsis*, for

example the commonly used Landsberg, will increase the noise to scoring the *coca* phenotype and therefore render map based cloning impossible. Therefore, we decided to adopt MutMap based cloning through whole genome resequencing and successfully mapped DRP1A as the causal mutation in *coca1*.

6.1.3 DRP1A mediate thermal perception through the modification of membrane curvature

Pharmacological studies of *DRP1A* indicated that it is upstream of membrane rigidification. DMSO treatment shows that the lipid composition in the WT and *coca1* are not significant different and therefore they both respond to DMSO triggered membrane rigidification similarly. Colchicine induced microtubule dissociation study showed that DRP1A also functions upstream of cytoskeleton re-organization. In summary, we propose that there are two possible working model of DRP1A in the perception of ambient cool temperatures.

In the first model, DRP1A senses low temperature and responds by homodimerization. The homodimerization triggers the GTP hydrolysis which generates a force against the plasma membrane it associates with. This leads to the modification of the membrane curvature, as is the case of DRP1A mediated endocytosis. This curvature in turn causes a conformational change in the calcium channel embedded in the plasma membrane, leading to its activation and subsequent cold induced $[Ca^{2+}]_i$ increase.

In the second model, DRP1A mediates endocytosis which regulates the transport and recycling of cold activated Ca^{2+} channels on the plasma membrane.

Through an unknown mechanism, this endocytosis related signaling leads to cold induced $[Ca^{2+}]_i$ increase.

6.2 Perspectives

6.2.1 Functional characterization

To test if DRP1A functions through endocytosis signaling, chemical inhibitors that specifically block endocytosis without affecting the function of DRP1A can be tested. The assumption is that if DRP1A mediated low temperature perception is achieved through impaired endocytosis, blocking endocytosis in WT should mimic the mutant phenotype of *coca1*. However, if the perception is achieved through DRP1A mediated membrane curvature, blocking endocytosis should not affect low temperature induced $[Ca^{2+}]_i$ increase in WT. Furthermore, *in vitro* GTP hydrolysis and dimerization of DRP1A in response to temperature could be performed, which will provide direct evidence that DRP1A is itself a temperature sensor whose activity can be directly modulated by temperature changes.

Additionally, map based cloning of other mutants should also be performed. This will provide a more complete picture of components involved in low temperature perception in plants.

Furthermore, providing that DRP1A has dual function of membrane curvature generation and endocytosis, an interesting question will be which domain of DRP1A is involved in temperature sensing and which domain is involved in endocytosis. Targeted mutation within the protein can be carried out to answer this question.

6.2.2 Improvement of agricultural crop

Potential application in crop improvement can be tested. Crop plants for example rice, corn and tomato homolog of DRP1A could be identified. Transgenic plants over-expressing DRP1A can be generated to see if increased fitness at low temperature can be achieved.

Alternatively, if the functional domain of DRP1A that separates its vesicle budding role from its temperature sensing role, protein engineering can be carried out using CRISPR Cas9 system and genetically engineer the protein to be more sensitive to temperature changes and even towards freezing temperatures.

References:

1 Fischer, E. M. & Knutti, R. Anthropogenic contribution to global occurrence of heavy-precipitation and high-temperature extremes. *Nat Clim Change* **5**, 560-+ (2015).

2 Thuiller, W., Lavorel, S., Araujo, M. B., Sykes, M. T. & Prentice, I. C. Climate change threats to plant diversity in Europe. *Proc Natl Acad Sci U S A* **102**, 8245-8250, doi:10.1073/pnas.0409902102 (2005).

3 Miura, K. & Furumoto, T. Cold Signaling and Cold Response in Plants. *Int J Mol Sci* **14**, 5312-5337, doi:10.3390/ijms14035312 (2013).

4 Knight, M. R. & Knight, H. Low-temperature perception leading to gene expression and cold tolerance in higher plants. *New Phytol* **195**, 737-751, doi:10.1111/j.1469-8137.2012.04239.x (2012).

5 Quint, M. *et al.* Molecular and genetic control of plant thermomorphogenesis. *Nat Plants* **2**, doi:Artn 15190

10.1038/Nplants.2015.190 (2016).

6 Gray, W. M., Ostin, A., Sandberg, G., Romano, C. P. & Estelle, M. High temperature promotes auxin-mediated hypocotyl elongation in Arabidopsis. *Proc Natl Acad Sci U S A* **95**, 7197-7202 (1998).

7 Crawford, A. J., McLachlan, D. H., Hetherington, A. M. & Franklin, K. A. High temperature exposure increases plant cooling capacity. *Current Biology* **22**, R396-R397 (2012).

8 Franklin, K. A. *et al.* Phytochrome-interacting factor 4 (PIF4) regulates auxin biosynthesis at high temperature. *Proc Natl Acad Sci U S A* **108**, 20231-20235, doi:10.1073/pnas.1110682108 (2011).

9 Koini, M. A. *et al.* High temperature-mediated adaptations in plant architecture require the bHLH transcription factor PIF4. *Current biology : CB* **19**, 408-413, doi:10.1016/j.cub.2009.01.046 (2009).

10 Christians, M. J., Gingerich, D. J., Hua, Z. H., Lauer, T. D. & Vierstra, R. D. The Light-Response BTB1 and BTB2 Proteins Assemble Nuclear Ubiquitin Ligases That Modify Phytochrome B and D Signaling in Arabidopsis. *Plant Physiology* **160**, 118-134, doi:10.1104/pp.112.199109 (2012).

11 Baulcombe, D. C. & Dean, C. Epigenetic regulation in plant responses to the environment. *Cold Spring Harbor perspectives in biology* **6**, a019471, doi:10.1101/cshperspect.a019471 (2014).

12 Kim, D. H., Doyle, M. R., Sung, S. & Amasino, R. M. Vernalization: Winter and the Timing of Flowering in Plants. *Annu Rev Cell Dev Bi* **25**, 277-299, doi:10.1146/annurev.cellbio.042308.113411 (2009).

13 Michaels, S. D. & Amasino, R. M. FLOWERING LOCUS C encodes a novel MADS domain protein that acts as a repressor of flowering. *Plant Cell* **11**, 949-956, doi:Doi 10.1105/Tpc.11.5.949 (1999).

14 Sung, S. B. & Amasino, R. M. Vernalization in Arabidopsis thaliana is mediated by the PHD finger protein VIN3. *Nature* **427**, 159-164, doi:10.1038/nature02195 (2004).

15 Gendall, A. R., Levy, Y. Y., Wilson, A. & Dean, C. The VERNALIZATION 2 gene mediates the epigenetic regulation of vernalization in Arabidopsis. *Cell* **107**, 525-535, doi:Doi 10.1016/S0092-8674(01)00573-6 (2001).

16 Greb, T. *et al.* The PHD finger protein VRN5 functions in the epigenetic silencing of Arabidopsis FLC. *Current Biology* **17**, 73-78, doi:10.1016/j.cub.2006.11.052 (2007).

17 Thomashow, M. F. Plant cold acclimation: Freezing tolerance genes and regulatory mechanisms. *Annual review of plant physiology and plant molecular biology* **50**, 571-599, doi:DOI 10.1146/annurev.arplant.50.1.571 (1999).

18 Ingram, J. & Bartels, D. The molecular basis of dehydration tolerance in plants. *Annual review of plant physiology and plant molecular biology* **47**, 377-403, doi:DOI 10.1146/annurev.arplant.47.1.377 (1996).

19 Thomashow, M. F. Role of cold-responsive genes in plant freezing tolerance. *Plant Physiology* **118**, 1-7, doi:Doi 10.1104/Pp.118.1.1 (1998).

20 Kiyosue, T., Yamaguchishinozaki, K. & Shinozaki, K. Characterization of 2 Cdnas (Erd10 and Erd14) Corresponding to Genes That Respond Rapidly to Dehydration Stress in Arabidopsis-Thaliana. *Plant Cell Physiol* **35**, 225-231 (1994).

21 Kovacs, D., Kalmar, E., Torok, Z. & Tompa, P. Chaperone activity of ERD10 and ERD14, two disordered stress-related plant proteins. *Plant Physiology* **147**, 381-390, doi:10.1104/pp.108.118208 (2008).

22 Yamaguchishinozaki, K. & Shinozaki, K. A Novel Cis-Acting Element in an Arabidopsis Gene Is Involved in Responsiveness to Drought, Low-Temperature, or High-Salt Stress. *Plant Cell* **6**, 251-264, doi:Doi 10.1105/Tpc.6.2.251 (1994).

23 Stockinger, E. J., Gilmour, S. J. & Thomashow, M. F. Arabidopsis thaliana CBF1 encodes an AP2 domain-containing transcriptional activator that binds to the C-repeat/DRE, a cis-acting DNA regulatory element that stimulates transcription in response to low temperature and water deficit. *P Natl Acad Sci USA* **94**, 1035-1040, doi:DOI 10.1073/pnas.94.3.1035 (1997).

24 Gilmour, S. J., Fowler, S. G. & Thomashow, M. F. Arabidopsis transcriptional activators CBF1, CBF2, and CBF3 have matching functional activities. *Plant molecular biology* **54**, 767-781, doi:Doi 10.1023/B:Plan.0000040902.06881.D4 (2004).

25 Gilmour, S. J., Sebolt, A. M., Salazar, M. P., Everard, J. D. & Thomashow, M. F. Overexpression of the Arabidopsis CBF3 transcriptional activator mimics multiple biochemical changes associated with cold acclimation. *Plant Physiology* **124**, 1854-1865, doi:DOI 10.1104/pp.124.4.1854 (2000).

26 Chinnusamy, V. *et al.* ICE1: a regulator of cold-induced transcriptome and freezing tolerance in Arabidopsis. *Gene Dev* **17**, 1043-1054, doi:10.1101/gad.1077503 (2003).

27 Dong, C. H., Agarwal, M., Zhang, Y. Y., Xie, Q. & Zhu, J. K. The negative regulator of plant cold responses, HOS1, is a RING E3 ligase that mediates the ubiquitination and degradation of ICE1. *P Natl Acad Sci USA* **103**, 8281-8286, doi:10.1073/pnas.0602874103 (2006).

28 Lee, H. J. *et al.* The Arabidopsis HOS1 gene negatively regulates cold signal transduction and encodes a RING finger protein that displays cold-regulated nucleo-cytoplasmic partitioning. *Gene Dev* **15**, 912-924, doi:Doi 10.1101/Gad.866801 (2001).

29 Catala, R. *et al.* The Arabidopsis E3 SUMO ligase SIZ1 regulates plant growth and drought responses. *Plant Cell* **19**, 2952-2966, doi:10.1105/tpc.106.049981 (2007).

30 Salome, P. A., Weigel, D. & McClung, C. R. The Role of the Arabidopsis Morning Loop Components CCA1, LHY, PRR7, and PRR9 in Temperature Compensation. *Plant Cell* **22**, 3650-3661, doi:10.1105/tpc.110.079087 (2010).

31 Portoles, S. & Mas, P. The Functional Interplay between Protein Kinase CK2 and CCA1 Transcriptional Activity Is Essential for Clock Temperature Compensation in Arabidopsis. *Plos Genet* **6**, doi:ARTN e1001201

10.1371/journal.pgen.1001201 (2010).

32 Chen, I. C., Hill, J. K., Ohlemuller, R., Roy, D. B. & Thomas, C. D. Rapid Range Shifts of Species Associated with High Levels of Climate Warming. *Science* **333**, 1024-1026, doi:10.1126/science.1206432 (2011).

33 Theurillat, J. P. & Guisan, A. Potential impact of climate change on vegetation in the European Alps: A review. *Climatic Change* **50**, 77-109, doi:Doi 10.1023/A:1010632015572 (2001).

34 Orvar, B. L., Sangwan, V., Omann, F. & Dhindsa, R. S. Early steps in cold sensing by plant cells: the role of actin cytoskeleton and membrane fluidity. *The Plant journal : for cell and molecular biology* **23**, 785-794 (2000).

35 Sangwan, V., Foulds, I., Singh, J. & Dhindsa, R. S. Cold-activation of Brassica napus BN115 promoter is mediated by structural changes in membranes and cytoskeleton, and requires Ca2+ influx. *Plant Journal* **27**, 1-12, doi:DOI 10.1046/j.1365-313x.2001.01052.x (2001).

36 Dodd, A. N., Kudla, J. & Sanders, D. The Language of Calcium Signaling. *Annu Rev Plant Biol* **61**, 593-620, doi:10.1146/annurev-arplant-070109-104628 (2010).

37 Carpaneto, A. *et al.* Cold transiently activates calcium-permeable channels in Arabidopsis mesophyll cells. *Plant Physiology* **143**, 487-494, doi:10.1104/pp.106.090928 (2007).

38 Plieth, C., Hansen, U. P., Knight, H. & Knight, M. R. Temperature sensing by plants: the primary characteristics of signal perception and calcium response. *Plant Journal* **18**, 491-497, doi:DOI 10.1046/j.1365-313X.1999.00471.x (1999).

39 Knight, H. & Knight, M. R. Recombinant aequorin methods for intracellular calcium measurement in plants. *Method Cell Biol* **49**, 201-216, doi:Doi 10.1016/S0091-679x(08)61455-7 (1995).

40 Knight, H., Trewavas, A. J. & Knight, M. R. Cold calcium signaling in Arabidopsis involves two cellular pools and a change in calcium signature after acclimation. *Plant Cell* **8**, 489-503, doi:10.1105/tpc.8.3.489 (1996).

41 Knight, M. R., Campbell, A. K., Smith, S. M. & Trewavas, A. J. Transgenic plant aequorin reports the effects of touch and cold-shock and elicitors on cytoplasmic calcium. *Nature* **352**, 524-526, doi:10.1038/352524a0 (1991).

42 Finka, A., Cuendet, A. F., Maathuis, F. J., Saidi, Y. & Goloubinoff, P. Plasma membrane cyclic nucleotide gated calcium channels control land plant thermal sensing and acquired thermotolerance. *Plant Cell* **24**, 3333-3348, doi:10.1105/tpc.112.095844 (2012).

43 Finka, A. & Goloubinoff, P. The CNGCb and CNGCd genes from Physcomitrella patens moss encode for thermosensory calcium channels

responding to fluidity changes in the plasma membrane. *Cell stress & chaperones* **19**, 83-90, doi:10.1007/s12192-013-0436-9 (2014).

44 Saijo, Y., Hata, S., Kyozuka, J., Shimamoto, K. & Izui, K. Over-expression of a single Ca2+-dependent protein kinase confers both cold and salt/drought tolerance on rice plants. *Plant Journal* **23**, 319-327, doi:DOI 10.1046/j.1365-313x.2000.00787.x (2000).

45 Townley, H. E. & Knight, M. R. Calmodulin as a potential negative regulator of Arabidopsis COR gene expression. *Plant Physiology* **128**, 1169-1172, doi:10.1104/pp.010814 (2002).

46 Huang, C. L., Ding, S., Zhang, H., Du, H. & An, L. Z. CIPK7 is involved in cold response by interacting with CBL1 in Arabidopsis thaliana. *Plant Sci* **181**, 57-64, doi:10.1016/j.plantsci.2011.03.011 (2011).

47 Doherty, C. J., Van Buskirk, H. A., Myers, S. J. & Thomashow, M. F. Roles for Arabidopsis CAMTA Transcription Factors in Cold-Regulated Gene Expression and Freezing Tolerance. *Plant Cell* **21**, 972-984, doi:10.1105/tpc.108.063958 (2009).

48 Janmey, P. A. The cytoskeleton and cell signaling: Component localization and mechanical coupling. *Physiol Rev* **78**, 763-781 (1998).

49 Mazars, C. *et al.* Organization of cytoskeleton controls the changes in cytosolic calcium of cold-shocked Nicotiana plumbaginifolia protoplasts. *Cell Calcium* **22**, 413-420 (1997).

50 Pokorna, J. *et al.* Sites of actin filament initiation and reorganization in cold-treated tobacco cells. *Plant Cell Environ* **27**, 641-653, doi:DOI 10.1111/j.1365-3040.2004.01186.x (2004).

51 Kumar, S. V. & Wigge, P. A. H2A.Z-containing nucleosomes mediate the thermosensory response in Arabidopsis. *Cell* **140**, 136-147, doi:10.1016/j.cell.2009.11.006 (2010).

52 Legris, M. *et al.* Phytochrome B integrates light and temperature signals in Arabidopsis. *Science* **354**, 897-900, doi:10.1126/science.aaf5656 (2016).

53 Jae-Hoon Jung, M. D., 1* Cornelia Klose,2* Surojit Biswas,1*† Daphne Ezer,1* Mingjun Gao,1 Asif Khan Khattak,3‡ Mathew S. Box,1 Varodom Charoensawan,1§ Sandra Cortijo,1 Manoj Kumar,1 Alastair Grant,3 James C. W. Locke,1,4 Eberhard Schäfer,2,5 Katja E. Jaeger,1 Philip A. Wigge1,6. Phytochromes function as thermosensors in Arabidopsis. *Science* (2016).

54 Chen, M., Tao, Y., Lim, J., Shaw, A. & Chory, J. Regulation of phytochrome B nuclear localization through light-dependent unmasking of nuclear-localization signals. *Current Biology* **15**, 637-642, doi:DOI 10.1016/j.cub.2005.02.028 (2005).

55 Sengupta, P. & Garrity, P. Sensing temperature. *Current Biology* **23**, R304-R307 (2013).

56 McKemy, D. D. Temperature sensing across species. *Pflugers Archiv : European journal of physiology* **454**, 777-791, doi:10.1007/s00424-006-0199-6 (2007).

57 Hunger, K., Beckering, C. L. & Marahiel, M. A. Genetic evidence for the temperature-sensing ability of the membrane domain of the Bacillus subtilis histidine kinase DesK. *FEMS microbiology letters* **230**, 41-46 (2004).

58 Albanesi, D., Mansilla, M. C. & de Mendoza, D. The membrane fluidity sensor DesK of Bacillus subtilis controls the signal decay of its cognate response regulator. *Journal of bacteriology* **186**, 2655-2663 (2004).

59 Suzuki, I., Los, D. A., Kanesaki, Y., Mikami, K. & Murata, N. The pathway for perception and transduction of low-temperature signals in Synechocystis. *Embo J* **19**, 1327-1334, doi:10.1093/emboj/19.6.1327 (2000).

60 Los, D. A. The effect of low-temperature-induced DNA supercoiling on the expression of the desaturase genes in synechocystis. *Cellular and molecular biology* **50**, 605-612 (2004).

61 Hedgecock, E. M. & Russell, R. L. Normal and mutant thermotaxis in the nematode Caenorhabditis elegans. *Proc Natl Acad Sci U S A* **72**, 4061-4065 (1975).

62 Mohri, A. *et al.* Genetic control of temperature preference in the nematode Caenorhabditis elegans. *Genetics* **169**, 1437-1450, doi:10.1534/genetics.104.036111 (2005).

63 Mori, I. & Ohshima, Y. Neural Regulation of Thermotaxis in Caenorhabditis-Elegans. *Nature* **376**, 344-348, doi:Doi 10.1038/376344a0 (1995).

64 Coburn, C. M. & Bargmann, C. I. A putative cyclic nucleotide-gated channel is required for sensory development and function in C-elegans. *Neuron* **17**, 695-706, doi:Doi 10.1016/S0896-6273(00)80201-9 (1996).

65 Komatsu, H., Mori, I., Rhee, J. S., Akaike, N. & Ohshima, Y. Mutations in a cyclic nucleotide-gated channel lead to abnormal thermosensation and chemosensation in C-elegans. *Neuron* **17**, 707-718, doi:Doi 10.1016/S0896-6273(00)80202-0 (1996).

66 Komatsu, H. *et al.* Functional reconstitution of a heteromeric cyclic nucleotide-gated channel of Caenorhabditis elegans in cultured cells. *Brain Res* **821**, 160-168 (1999).

67 Inada, H. *et al.* Identification of guanylyl cyclases that function in thermosensory neurons of Caenorhabditis elegans. *Genetics* **172**, 2239-2252, doi:10.1534/genetics.105.050013 (2006).

68 Sayeed, O. & Benzer, S. Behavioral genetics of thermosensation and hygrosensation in Drosophila. *P Natl Acad Sci USA* **93**, 6079-6084, doi:DOI 10.1073/pnas.93.12.6079 (1996).

69 Tracey, W. D., Wilson, R. I., Laurent, G. & Benzer, S. painless, a Drosophila gene essential for nociception. *Cell* **113**, 261-273, doi:Doi 10.1016/S0092-8674(03)00272-1 (2003).

70 Montell, C. *et al.* A unified nomenclature for the superfamily of TRP cation channels. *Mol Cell* **9**, 229-231, doi:Doi 10.1016/S1097-2765(02)00448-3 (2002).

71 Viswanath, V. *et al.* Ion channels - Opposite thermosensor in fruitfly and mouse. *Nature* **423**, 822-823, doi:10.1038/423822a (2003).

72 Rosenzweig, M. *et al.* The Drosophila ortholog of vertebrate TRPA1 regulates thermotaxis. *Gene Dev* **19**, 419-424, doi:10.1101/gad.1278205 (2005).

73 Lee, Y. *et al.* Pyrexia is a new thermal transient receptor potential channel endowing tolerance to high temperatures in Drosophila melanogaster. *Nat Genet* **37**, 305-310, doi:10.1038/ng1513 (2005).

74 Hong, S. T. *et al.* Histamine and its receptors modulate temperature-preference behaviors in Drosophila. *J Neurosci* **26**, 7245-7256, doi:10.1523/Jneurosci.5426-05.2006 (2006).

75 Caterina, M. J. *et al.* The capsaicin receptor: a heat-activated ion channel in the pain pathway. *Nature* **389**, 816-824, doi:10.1038/39807 (1997).

76 Tominaga, M. *et al.* The cloned capsaicin receptor integrates multiple pain-producing stimuli. *Neuron* **21**, 531-543, doi:Doi 10.1016/S0896-6273(00)80564-4 (1998).

77 Caterina, M. J. *et al.* Impaired nociception and pain sensation in mice lacking the capsaicin receptor. *Science* **288**, 306-313, doi:DOI 10.1126/science.288.5464.306 (2000).

78 McKemy, D. D., Neuhausser, W. M. & Julius, D. Identification of a cold receptor reveals a general role for TRP channels in thermosensation. *Nature* **416**, 52-58, doi:Doi 10.1038/Nature719 (2002).

79 Peier, A. M. *et al.* A TRP channel that senses cold stimuli and menthol. *Cell* **108**, 705-715, doi:Doi 10.1016/S0092-8674(02)00652-9 (2002).

80 Caterina, M. J., Rosen, T. A., Tominaga, M., Brake, A. J. & Julius, D. A capsaicin-receptor homologue with a high threshold for noxious heat. *Nature* **398**, 436-441 (1999).

81 Guler, A. D. *et al.* Heat-evoked activation of the ion channel, TRPV4. *J Neurosci* **22**, 6408-6414 (2002).

82 Jordt, S. E., McKemy, D. D. & Julius, D. Lessons from peppers and peppermint: the molecular logic of thermosensation. *Curr Opin Neurobiol* **13**, 487-492, doi:10.1016/S0959-4388(03)00101-6 (2003).

83 Gracheva, E. O. *et al.* Ganglion-specific splicing of TRPV1 underlies infrared sensation in vampire bats. *Nature* **476**, 88-91, doi:10.1038/nature10245 (2011).

84 Gracheva, E. O. *et al.* Molecular basis of infrared detection by snakes. *Nature* **464**, 1006-U1066, doi:10.1038/nature08943 (2010).

85 Ishitani, M., Xiong, L. M., Lee, H. J., Stevenson, B. & Zhu, J. K. HOS1, a genetic locus involved in cold-responsive gene expression in Arabidopsis. *Plant Cell* **10**, 1151-1161 (1998).

86 Shimomura, O., Johnson, F. H. & Morise, H. Mechanism of the luminescent intramolecular reaction of aequorin. *Biochemistry* **13**, 3278-3286 (1974).

87 Yuan, F. *et al.* OSCA1 mediates osmotic-stress-evoked Ca2+ increases vital for osmosensing in Arabidopsis. *Nature* **514**, 367-371, doi:10.1038/nature13593 (2014).

88 Monshausen, G. B., Messerli, M. A. & Gilroy, S. Imaging of the Yellow Cameleon 3.6 indicator reveals that elevations in cytosolic Ca(2+) follow oscillating increases in growth in root hairs of arabidopsis. *Plant Physiology* **147**, 1690-1698, doi:10.1104/pp.108.123638 (2008).

89 Costa, A., Candeo, A., Fieramonti, L., Valentini, G. & Bassi, A. Calcium Dynamics in Root Cells of Arabidopsis thaliana Visualized with Selective Plane Illumination Microscopy. *Plos One* **8**, doi:ARTN e75646

10.1371/journal.pone.0075646 (2013).

90 Kanchiswamy, C. N., Malnoy, M., Occhipinti, A. & Maffei, M. E. Calcium Imaging Perspectives in Plants. *Int J Mol Sci* **15**, 3842-3859, doi:10.3390/ijms15033842 (2014).

91 Nagai, T., Yamada, S., Tominaga, T., Ichikawa, M. & Miyawaki, A. Expanded dynamic range of fluorescent indicators for Ca2+ by circularly permuted yellow fluorescent proteins. *P Natl Acad Sci USA* **101**, 10554-10559, doi:DOI 10.1073/pnas.0400417101 (2004).

92 Kiegle, E., Moore, C. A., Haseloff, J., Tester, M. A. & Knight, M. R. Cell-type-specific calcium responses to drought, salt and cold in the Arabidopsis root. *The Plant journal : for cell and molecular biology* **23**, 267-278 (2000).

93 Han, S. C., Tang, R. H., Anderson, L. K., Woerner, T. E. & Pei, Z. M. A cell surface receptor mediates extracellular Ca2+ sensing in guard cells. *Nature* **425**, 196-200, doi:10.1038/nature01932 (2003).

94 Abe, A. *et al.* Genome sequencing reveals agronomically important loci in rice using MutMap. *Nature biotechnology* **30**, 174-178, doi:10.1038/nbt.2095 (2012).

95 Ferguson, S. M. & De Camilli, P. Dynamin, a membrane-remodelling GTPase. *Nat Rev Mol Cell Bio* **13**, 75-88, doi:10.1038/nrm3266 (2012).

96 Gasper, R., Meyer, S., Gotthardt, K., Sirajuddin, M. & Wittinghofer, A. It takes two to tango: regulation of G proteins by dimerization. *Nat Rev Mol Cell Bio* **10**, 423-429, doi:10.1038/nrm2689 (2009).

97 Byrnes, L. J. & Sondermann, H. Structural basis for the nucleotide-dependent dimerization of the large G protein atlastin-1/SPG3A. *P Natl Acad Sci USA* **108**, 2216-2221, doi:10.1073/pnas.1012792108 (2011).

98 Chappie, J. S. *et al.* A Pseudoatomic Model of the Dynamin Polymer Identifies a Hydrolysis-Dependent Powerstroke. *Cell* **147**, 209-222, doi:10.1016/j.cell.2011.09.003 (2011).

99 Minami, A. *et al.* Alterations in detergent-resistant plasma membrane microdomains in Arabidopsis thaliana during cold acclimation. *Plant Cell Physiol* **50**, 341-359, doi:10.1093/pcp/pcn202 (2009).

100 Whalley, H. J. *et al.* Transcriptomic Analysis Reveals Calcium Regulation of Specific Promoter Motifs in Arabidopsis. *Plant Cell* **23**, 4079-4095, doi:10.1105/tpc.111.090480 (2011).

101 Shpetner, H. S. & Vallee, R. B. Identification of Dynamin, a Novel Mechanochemical Enzyme That Mediates Interactions between Microtubules. *Cell* **59**, 421-432, doi:Doi 10.1016/0092-8674(89)90027-5 (1989).

102 Obar, R. A., Collins, C. A., Hammarback, J. A., Shpetner, H. S. & Vallee, R. B. Molecular-Cloning of the Microtubule-Associated Mechanochemical Enzyme Dynamin Reveals Homology with a New Family of Gtp-Binding Proteins. *Nature* **347**, 256-261, doi:Doi 10.1038/347256a0 (1990).

103 Grigliatti, T. A., Hall, L., Rosenbluth, R. & Suzuki, D. T. Temperature-Sensitive Mutations in Drosophila-Melanogaster .14. Selection of Immobile Adults. *Mol Gen Genet* **120**, 107-114, doi:Doi 10.1007/Bf00267238 (1973).

104 Vanderbliek, A. M. & Meyerowitz, E. M. Dynamin-Like Protein Encoded by the Drosophila-Shibire Gene Associated with Vesicular Traffic. *Nature* **351**, 411-414, doi:Doi 10.1038/351411a0 (1991).

105 Littleton, J. T. *et al.* Temperature-sensitive paralytic mutations demonstrate that synaptic exocytosis requires SNARE complex assembly and disassembly. *Neuron* **21**, 401-413, doi:Doi 10.1016/S0896-6273(00)80549-8 (1998).

106 Hinshaw, J. E. & Schmid, S. L. Dynamin Self-Assembles into Rings Suggesting a Mechanism for Coated Vesicle Budding. *Nature* **374**, 190-192, doi:Doi 10.1038/374190a0 (1995).

107 Hong, Z. *et al.* A unified nomenclature for Arabidopsis dynamin-related large GTPases based on homology and possible functions. *Plant molecular biology* **53**, 261-265, doi:Doi 10.1023/B:Plan.0000007000.29697.81 (2003).

108 Smith, J. M. *et al.* Loss of Arabidopsis thaliana Dynamin-Related Protein 2B reveals separation of innate immune signaling pathways. *PLoS pathogens* **10**, e1004578, doi:10.1371/journal.ppat.1004578 (2014).

109 Minami, A. *et al.* Arabidopsis dynamin-related protein 1E in sphingolipid-enriched plasma membrane domains is associated with the development of freezing tolerance. *The Plant journal : for cell and molecular biology* **83**, 501-514, doi:10.1111/tpj.12907 (2015).

110 Albert, E. S. *et al.* TRPV4 channels mediate the infrared laser-evoked response in sensory neurons. *J Neurophysiol* **107**, 3227-3234, doi:10.1152/jn.00424.2011 (2012).

Biography

Yan Xue was born in Shanghai, China. She studied Biology in The Chinese University of Hong Kong where she obtained her Bachelor of Science degree and developed her interest in plants. After spending two years studying plant disease resistance, she obtained her Master of Science degree at the same university. In 2009, she was admitted to the Ph.D. program at Duke University and joined Dr. Zhenming Pei's group where she studied plant thermal. She completed her dissertation and defense in 2017. Here is a list of publications she has worked on or contributed to.

Xue, Y., Xu, S.J., Yuan, F., Fan, Y.P., Huang, X., Liu, F., Ye, R. & Pei, Z.M. A novel function of DRP1A in mediating temperature perception in *Arabidopsis*. (In preparation to *Nature*)

Yuan, F., Yang, H.M.*, **Xue, Y.***, Kong, D.D., Ye, R., Li, C.J., Zhang, J.Y., Theprungsirikul, L., Shrift, T., Krichilsky, B., Johnson, D.M., Swift, G.B., He, Y.K., Siedow, J.N. & Pei Z.M. OSCA1 mediates osmotic-stress-evoked Ca2+ increases vital for osmosensing in *Arabidopsis. Nature.* **514:**367-371. (2014) (* equal contribution)

Cheung, M.Y., **Xue, Y.**, Zhou, L., Li, M.W., Sun, S.S.M & Lam, H.M. An ancient P-loop GTPase in rice is regulated by a higher plant-specific regulatory protein. *J. Biol. Chem.* **285**:37359–37369. (2010)

Cheung, M.Y., Zeng, N.Y., Tong, S.W., Li, F.W.Y., **Xue, Y.**, Zhao, K.J., Wang, C., Zhang, Q., Fu, Y., Sun, S.S.M. & Lam, H.M. Constitutive expression of a rice GTPase activating protein induces defense responses. *New Phytol*. **179**:530-545. (2008)